Wetting Front Instability in Uniform Soils Under Low Infiltration Rates

by

Tzung-mow Yao
New Mexico Institute of Mining and Technology

August 1993

Submitted in partial fulfillment of the requirements for
the degree of Master of Science in Hydrology

TABLE OF CONTENTS

LIST OF FIGURES IN CHAPTER 2

LIST OF TABLES IN CHAPTER 2

ACKNOWLEDGEMENT

I wish to express my gratitude to the New Mexico Water Resources Research Institute (NMWRRI) and Chino Mines for funding this project. I am also grateful for the large quantities of dry, clean perlite sand donated by the Grefco Mine at Socorro.

I would like to thank all the professors in the Hydrology Division for all the help and the knowledge conveyed. I offer special thanks to my advisor Dr. Jan Hendrickx for his generous support and patient advice. I am also grateful to Dr. William Stone for helping with the mathematical modeling, to Dr. Robert Lee for important reference material, and to Mr. Irl Downes for all his generous help.

I am indebted to the laboratory crew -- Steve Bower, Jay Cabrales, Craig Stevenson, and Kelly Kriel -- for their enthusiastic involvement and hard work in the lab.

Finally, I dedicate this work to my lovely wife and to my parents who have given me their support and understanding throughout my life.

Chapter 1

SYNOPSIS

SYNOPSIS

This thesis consists of a manuscript to be submitted to the Soil Science Society of America Journal along with various appendices. The research puts emphasis on wetting front instability under low infiltration rates that are similar to natural precipitation rates in New Mexico and elsewhere in the United States. The results of this study give an insight into the conditions under which preferential flow paths may occur in field soils. Such understanding is necessary for the determination of the vulnerability of the shallow groundwater aquifers to contamination.

The investigations reported in this study have focused on laboratory experiments that simulate field conditions. During the course of these laboratory experiments, a mathematical model to analyze the stability of wetting fronts was developed by Drs. William Stone and Jan Hendrickx and their students.

Future research will be supported by the National Science Foundation and will concentrate on field experiments and computer modeling.

Appendix A contains the results from water retention measurements on perlite sand. The RETC curve-fitting program (van Genuchten et al., 1991) was used to derive the van Genuchten parameters from these measurements. The mathematical model developed by Stone and Hendrickx (1993) uses those parameters as input parameters. Appendix B presents the results from the lysimeter experiments. The experimental conditions and visual inspection results are recorded. Appendix C contains the water content measurements and bulk density of the lysimeter experiments. Appendix D contains the sorptivity measurements for the perlite sands. Appendix E contains information on the

sprinkler system (rainfall simulator), including the design, sprinkler pattern and a distribution analysis of the artificial precipitation.

Chapter 2

Paper Titled "Wetting Front Instability in Uniform Soils Under Low Infiltration Rates"

by Tzung-mow Yao and Jan M.H. Hendrickx

To be submitted for publication in the Soil Science Society of America Journal

ABSTRACT

Lysimeter experiments were conducted in the laboratory to validate current wetting front instability theories. Four different grades of sieved and air-dried perlite sand were used as the experimental material. Water was applied by a sprinkler system at rates within the range of natural precipitation rates in the U.S.A.. Experiments were conducted in small lysimeters (diameter 30 cm, height 50 cm) as well as a large one (diameter 100 cm, height 150 cm).

The experimental results show that wetting front instability will cause fingering phenomena in a single layer soil system. This observation confirms experimental and theoretical results of other workers. The diameter of fingers is a function of the grain size of the sand. Small fingers (3-4 cm diameter) were found in coarse sand (14-20 mesh); large diameter fingers (12 cm diameter) were observed in the fine sand (40-60 mesh).

Our experimental results in the 14-20 sand show that, for infiltration rates varying between 0.3 and 12 cm/hour, finger diameters remain more or less constant. This agrees with existing theories. Our experimental results also show that, for infiltration rates lower than 0.12 cm/hour, the wetting fronts become stable. For rates between 0.3 and 0.12 cm/hour, the wetting is semi-stable; that is, there is incomplete wetting without distinct development of fingers. A similar trend can also be observed through the experimental results of 20-30 and 30-40 sand. This phenomenon has not been addressed in previous studies. Our experimental data under low infiltration rates support a recent general stability analysis of wetting fronts by Stone and Hendrickx (1993) that predicts wetting front behavior from very low infiltration rates to rates equal to the saturated conductivity of the sands.

INTRODUCTION

Worldwide, preferential flow paths are a major mechanism for groundwater contamination. These paths can be caused by macropores such as soil cracks or old root channels (Bouma, 1980; Beven and Germann, 1982), spacial variability of hydraulic conductivity, or by unstable wetting fronts. The occurrence of unstable fronts is of special importance because they may cause preferential flow paths in homogeneous soils without macropores or without large variability of hydraulic properties. This wetting front instability has been demonstrated by theoretical studies (Diment and Watson, 1983; Diment et al., 1982; Glass et al., 1989a, c, 1991; Hillel and Baker, 1988; Parlange and Hill, 1976; Philip, 1975a, b; Raats, 1973; Stone and Hendrickx, 1993; Tabuchi, 1961), laboratory experiments (Baker and Hillel, 1990; Diment and Watson, 1985; Glass et al., 1989b, 1990; Hendrickx et al., 1988a; Hill and Parlange, 1972; Selker et al., 1989, 1992; Tamai et al., 1987; White et al., 1976) and field investigations (Hendrickx et al., 1988b; Hendrickx and Dekker, 1991; Hendrickx et al. 1993; Ritsema et al. 1993; Van Ommen et al., 1989).

Theories to explain for unstable wetting in homogeneous soils have been presented by Raats (1973), Philip (1975a, b), Parlange and Hill (1976), Diment et al. (1982), Glass et al. (1989a, 1991), and recently by Stone and Hendrickx (1993). Based on the instability criterion for homogeneous soils, these theories have predicted instabilities to occur under the following conditions: (1) infiltration of ponded water with compression of air ahead of the wetting front; (2) redistribution of water in the soil profile; (3) water repellent soils; (4) an increase of water content with depth; and (5) continuous nonponding infiltration. In the case of continuous nonponding infiltration, Raats (1973) and Stone and Hendrickx (1993) predicted instabilities to occur, whereas Philip (1975a) predicted that none would

occur. Experimental evidence, however, shows that instabilities do occur in single-layer homogeneous soils during nonponding infiltration (Hagerman et al., 1989; Hendrickx and Dekker, 1991; Selker et al., 1989, 1992; Yao and Hendrickx, 1993).

The diameter of the preferential flow paths or fingers, has been studied through stability analysis by Philip (1975a, b), Parlange and Hill (1976) and Glass et. al. (1991). These researchers have stated that the critical wavelength necessary to induce unstable wetting yields an estimate of the finger diameter. However, the critical wavelength may not represent the dominant or average finger size. Glass et al. (1989a, b; 1991) derived a formula for finger diameter in two- and three-dimensional systems. For three-dimensions:

$$d=4.8\frac{S_w^2}{K_s(\theta_s-\theta_0)}\left[\frac{1}{1-q_s/K_F}\right]\cdots\cdots\cdots(1)$$

where d is the diameter of the fingers, S_w is the sorptivity of the porous medium at water entry value, K_s is the saturated hydraulic conductivity, θ_s is the saturated water content, θ_0 is the initial water content, q_s is the infiltration rate and 4.8 is a coefficient derived from stability analysis (Glass et al. 1991). K_F is the hydraulic conductivity inside the finger, a value is assumed to be close to K_s.

This formula indicates that the finger diameter will increase in finer soils because they generally have a higher sorptivity and lower saturated conductivity. It also indicates that the finger diameter will increase with increasing infiltration rates until the wetting fronts become stable at infiltration rates equal to or higher than the saturated hydraulic conductivity of the soil. For infiltration rates approaching zero, the formula predicts a constant small finger diameter, indicating the persistence of unstable wetting under these

low rates. Selker et al. (1992) and Glass et al. (1989b, 1990) have presented experimental data to support the formula for higher infiltration rates.

The stability analysis of Stone and Hendrickx (1993) also predicts stable wetting fronts in finer soils and at infiltration rates approaching the saturated hydraulic conductivity. However, contrary to the formula of Glass et al. (1989a, b), their analysis predicts stable wetting fronts when the infiltration rates become low.

Because to date no studies have been carried out to investigate the mechanism of unstable wetting in initially dry, wettable homogeneous soils under low infiltration rates, the objective of this study is to investigate the mechanism of unstable wetting under these conditions.

MATERIALS AND METHODS

Experimental Sands

For this study we used four different grades: U.S. mesh size No. 14-20 (1.41-.841mm), 20-30 (.841-.594mm), 30-40 (.594-.42mm), and 40-60 (.42-.25mm). The particle size distribution was determined with a sieve analysis (Fig. 1). The uniformity coefficients ranged from 1.18 to 1.37 and indicated that the sands were quite homogeneous. For our experiments we needed to transport, dry, clean, and sieve approximately 10 m^3 sand.

Physical Parameters of the Sand

Perlite is similar to quartz sand, but has a lower specific density of approximately 2.2 g/cm^3. This leads to a bulk density in the lysimeters of approximately 1.25 g/cm^3 and a porosity of 45%.

For each grade we determined two water retention curves with the hanging water column technique on 100 cm^3 dry samples that were taken in-situ from the lysimeters. The data from both samples were simultaneously fit by a revised version of the RETC program (van Genuchten et al. 1991). The hydraulic conductivity was measured with the constant head method. Water-entry values were estimated gravimetrically from vertical capillary rise experiments (Glass et al., 1990). The sand was packed into a 10 cm diameter PVC column consisting of twenty rings, each 1 cm high. The bottom part of this column was immersed into water for one day. Next, the water content of each 1 cm layer was measured. After plotting the water contents versus the average height of the samples, water-entry values were determined, by definition, at the lowest point of water tension along the saturation portion of the wetting curve (Glass et al., 1989c). We also

Fig. 1 Grain Size Distribution of Perlite Sand.

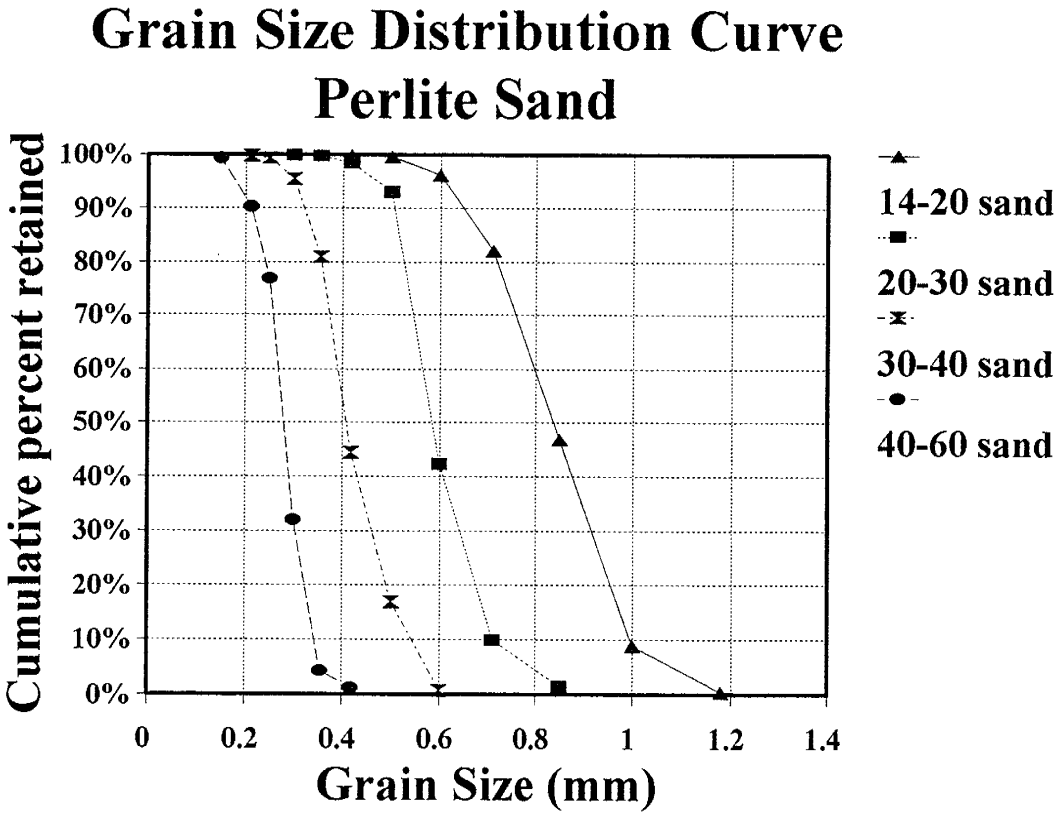

determined water-entry values by fitting the wetting curve using the RETC program with the Brooks and Corey equation. The sorptivities of the sand at the water entry value were determined with a tension infiltrometer (Ankeny et al., 1988).

There was some concern that the chemically bound water molecules of the perlite could be set free during drying of samples in the stove. However, tests revealed this was not the case: perlite behaves like any other sand.

Lysimeter Experiments

The air-dried perlite sands were used to fill small and large non-weighing lysimeters, with diameters of, respectively, 30 and 100 cm and heights of 50 and 150 cm. The small lysimeters were designed after those employed by Glass et al. (1990). A funnel-extension-randomizer also based on the design of Glass et al. (1990) randomized the falling sand so that microlayering and grading due to particle size segregation was avoided. We filled seven rings with sand. After filling, the top two layers were taken off and the surface of the column was smoothed.

In order to study fingers with diameters larger than 30 cm, we used a large lysimeter (Fig. 2) which, in this case, consisted of 10 circular slabs, each 15 cm high. The inside diameter of the lysimeter was 100 cm. The bottom slab was divided into 45 compartments with dimensions of 10x10 cm. Some compartments at the side of the lysimeter were smaller than 10x10 cm. The height of each of the compartments was 15 cm. This height was sufficient to prevent flow from one compartment into another. Each of the compartments had its own outlet to measure the drainage volume. The bottom slab was 50 cm above the floor level for easy access to and control of the 45 drainage outlets. A strong support was constructed to carry the weight of the lysimeter filled with sand and

Fig. 2 Design of the Large Lysimeter.

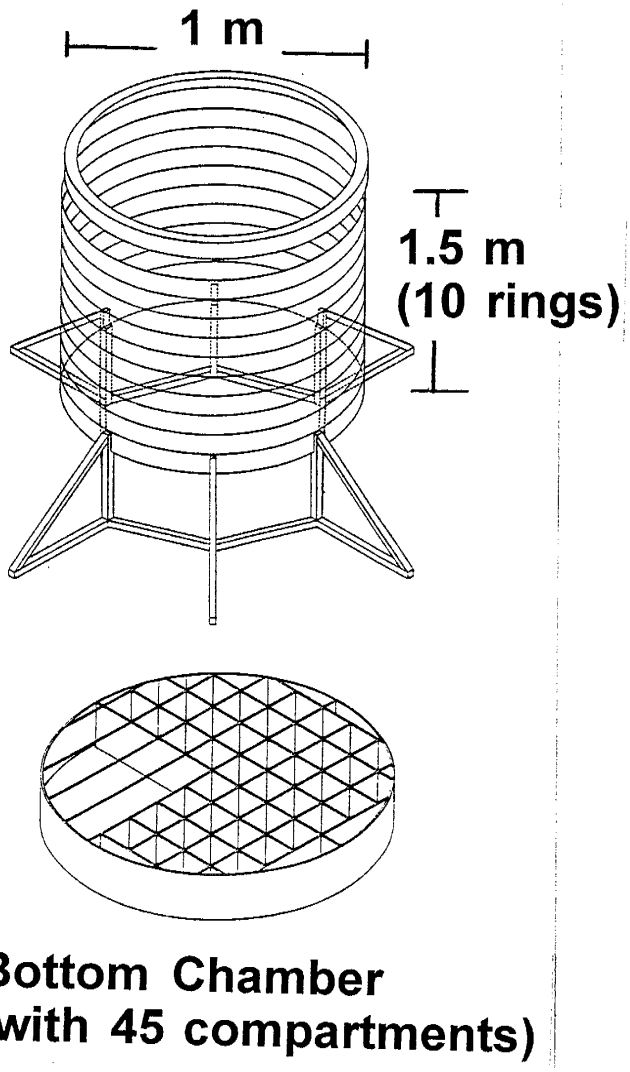

water. The slabs, with a gasket in between, were bolted together so that a water- and air-tight connection was obtained. The 45 outlets in the bottom prevented the air pressure from increasing during the infiltration experiments.

To fill the large lysimeter with perlite sands, we used a 1 m diameter "funnel-extension-randomizer" as described above. In addition, a chute was built to make the filling process more convenient. The entire experimental setup involved two stories in our laboratory.

Water Application

A sprinkler system with a uniform water application was built. Eleven hundred drip needles were uniformly inserted in a sealed plexi-glass box at grid points 3 cm apart. The needles covered a circular area with a 1.2 m diameter. The drop size from the needles (20 G1, from Beckon and Dickenson) was measured as 3 mm in diameter, which is close to the drop size of a storm rainfall in the United States (Bubenzer, 1979; Carter et al., 1974; Laws and Parsons, 1943). Two variable-speed, low gear motors were placed on two adjoining sides to control the north-south and east-west movements separately. The offsets in both directions could be adjusted so that we could obtain a random distribution of the water without a regular pattern. A Masterflex pump was used for very accurate flow control and the sprinkler rate could be adjusted from 0.12 cm/hour to 36 cm/hour.

The lysimeters were exposed to infiltration regimes with different application rates and amounts of water. We used application rates and total amounts of water that are representative for natural precipitation events in New Mexico and elsewhere in the world (Bubenzer, 1979). The infiltration rates varied between 0.12 cm/hour to 27 cm/hour; the total amounts between 2.5 to 8 cm.

After water application, the lysimeters were excavated layer by layer to allow us to visually inspect the flow pattern. Samples were taken within and outside the fingers to determine bulk density and water content. In each layer we photographed the wetting pattern for later analysis of total wet area and finger diameter. Ninety-two experiments were conducted in initially dry sands under the experimental conditions shown in Table 1.

Table 1. Summary of Experiments

	Sand size							
	14-20		20-30		30-40		40-60	
	Lysimeter type[†]							
Infiltration rate	S	L	S	L	S	L	S	L
(cm/hour)								
0.12- 0.5	6		5		5		3	
0.5- 3.0	4		3		4	1	4	
3.0- 6.0	9	1	6		2	1	2	1
6.0- 9.0	14		1			1		
9.0-12.0	9					1		
12.0<	1		2		2		3	1
Total experiments	43	1	17	0	13	4	12	2

[†] S means small lysimeter; L means large lysimeter.

RESULTS AND DISCUSSION

Effect of Sand Grain Size on Finger Diameter

The results of the soil physical measurements are presented in Table 2. As expected, the saturated conductivity decreases if the sand becomes finer, whereas the sorptivity, in general, increases. The sorptivity at water-entry tension was estimated by interpolating the plot of sorptivities versus tensions. The high variability of the sorptivity values in the region close to the water-entry tension makes interpolation difficult and may have resulted in the lower sorptivity values for the 40-60 sand.

Glass et al. (1991) stated that, when the ratio R_s (infiltration rate/ saturated hydraulic conductivity) becomes smaller than 0.5, the finger sizes for his soils varied only slightly. Visual inspection of our experiments at infiltration rates between 0.3 and 12 cm/hour revealed that fingering is always occurring in a single layer of soil. The fingers join quite often and the total number of the fingers is hard to determine. However, there are still enough independent fingers to allow us to determine finger sizes. Figures 3A- 3D show experimental results for different sand sizes at a depth of 30 cm under similar water application rates. Fig. 3A shows the results of 14-20 sand under an application rate of 9 cm/hour with finger diameters of 3-4 cm. Fig. 3B shows 20-30 sand under 4.26 cm/hour with finger diameters of 5-6 cm. Fig. 3C shows 30-40 sand under 12.3 cm/hour with finger diameters of 6-10 cm. Fig. 3D shows 40-60 sand under 9 cm/hour with finger diameters of 8-15 cm. It is very clear that the finger diameter increases with decreasing grain size. This trend was successfully predicted by equation (1) (Glass et al., 1991).

Table 2. Physical Parameters of the Perlite Sand

Parameters									
Sand size	K_s	θ_s	θ_r	α	n	$\Psi_{we}^{\dagger}$	$\Psi_{we}^{\ddagger}$	$S^{\dagger}$	$S^{\ddagger}$
U.S.mesh	cm/sec			1/cm		cm	cm	$cm/sec^{1/2}$	
14-20	.33	.45	.075	.188	3.48	3.55	3.5	.22	.22
20-30	.20	.45	.044	.131	4.5	5.1	6.0	.38	.28
30-40	.13	.45	.063	.092	5.07	7.3	8.0	.39	.29
40-60	.07	.45	.052	.062	5.19	11.4	10.0	.15	.25

θ_s: Saturated water content.

θ_r: Residual water content.

α, n: Empirical parameters that describe the shape of the water retention curve in the V-G equation.

$\Psi_{we}^{\dagger}$: Water-entry value based on the fitting of the Brooks and Corey equation.

$\Psi_{we}^{\ddagger}$: Water-entry value based on the capillary rise experiments.

$S^{\dagger}$: Sorptivity at water-entry value based on the fitting of the Brooks and Corey equation.

$S^{\ddagger}$: Sorptivity at water-entry value based on the capillary rise experiments.

Fig. 3. Experimental Results at High Infiltration Rates.

A. 14-20 Sand
(in small lysimeter, 30 cm in diameter)

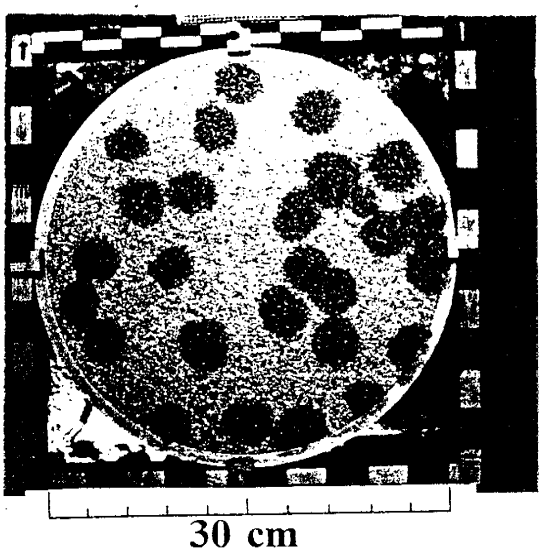

B. 20-30 Sand
(in small lysimeter, 30 cm in diameter)

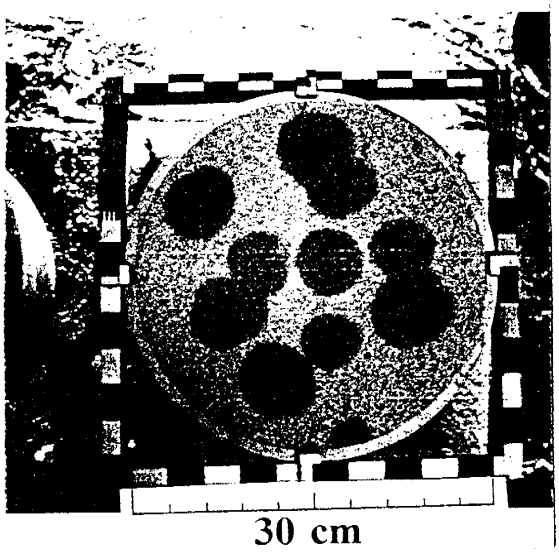

C. 30-40 Sand
(in large lysimeter, 1 m in diameter)

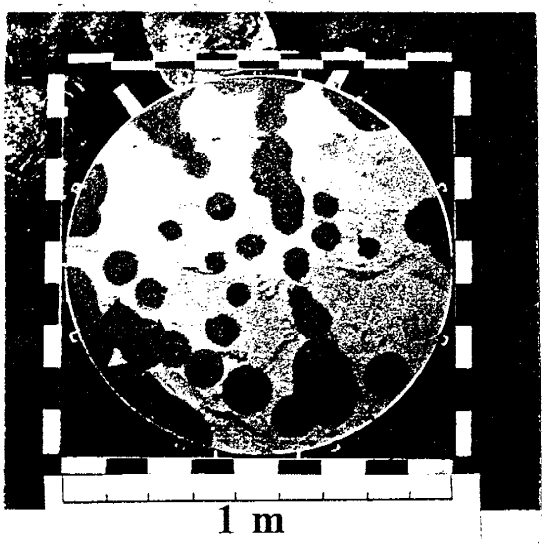

D. 40-60 Sand
(in large lysimeter, 1 m in diameter)

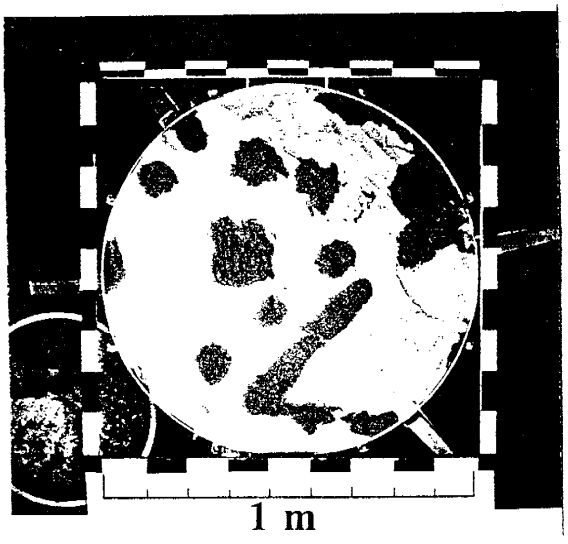

The number of fingers decreases when the grain size decreases. However, it is not clear whether grain size of the soils has any relationship with the wetting ratio (wet area /total area for a horizontal cross-section of the column). For our experiments the wetting ratio falls in the range of 20-40% under high water application regimes (0.5 cm/hour - 27 cm/hour).

Effect of Decreasing Infiltration Rates on Finger Diameter

The experimental results are summarized in Fig. 4 and the finger diameters predicted by Eq. (1) are also shown. It is clear that this formula fails to provide a prediction of finger diameter at low water infiltration rates. The two finger diameter of 30 cm indicates stable wetting, because these fingers cover the entire horizontal cross section of the small lysimeters. Fig. 5A and Fig. 5B show the results of 14-20 sand experiments under high infiltration rates. Fig 5A shows the highest rate (9 cm/hour) and has finger diameters of 2.5-4 cm. Fig. 5B shows a rate of 3.2 cm/hour and has finger diameters of 4-6 cm. Fig 5C and Fig. 5D show results under very low infiltration rate conditions; very large fingers and incomplete wetting are observed.

The low infiltration rate experiments are important to an understanding of unstable wetting under natural conditions since they simulate the conditions at a low precipitation rate or where a coarse layer is overlaid by a fine soil layer. Figures 5A-5D show a trend of widening finger diameters at low infiltration rates. For our 30 cm diameter column, the finger diameters start to increase below a rate of 1 cm/hour and stabilize at the rate of 0.12 cm/hour (Fig. 5D). For fine grain size sand the stabilization appears to start at

Fig. 4. Plot of Finger Diameters vs. the Infiltration Rates.

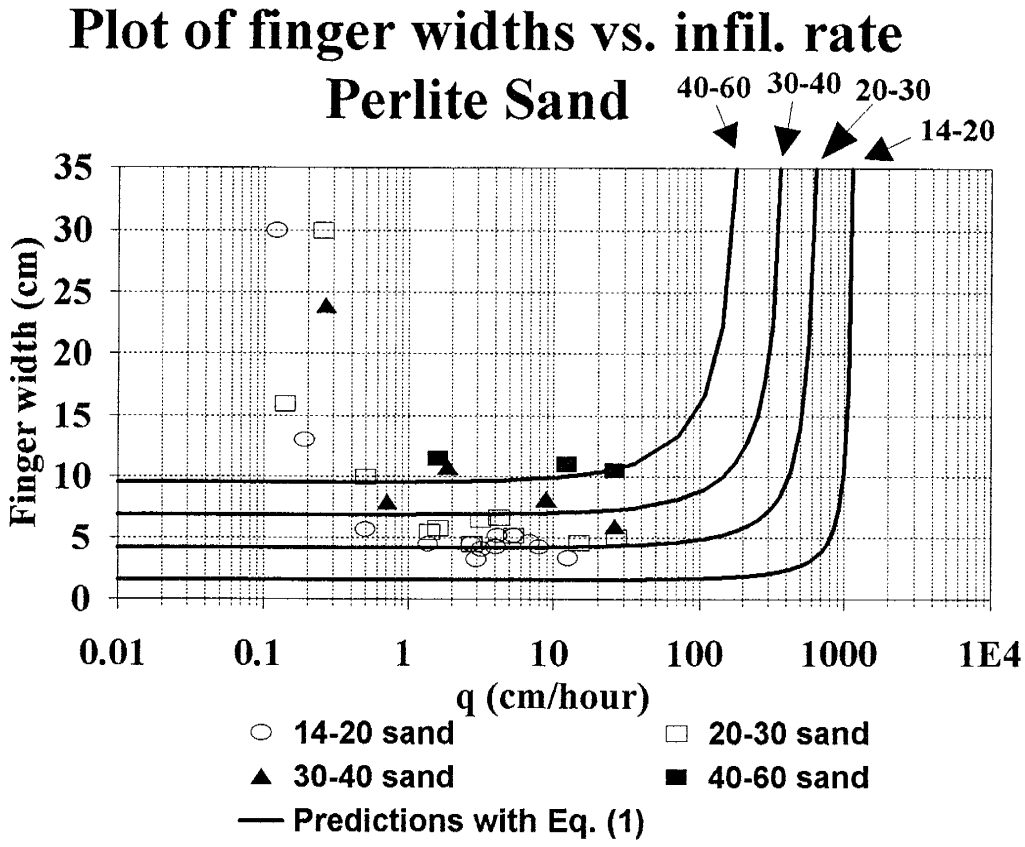

Fig. 5. Experimental Results of 14-20 Sand at High and Low Infiltration Rates.

A. High Infiltration Rate (9cm/hour)

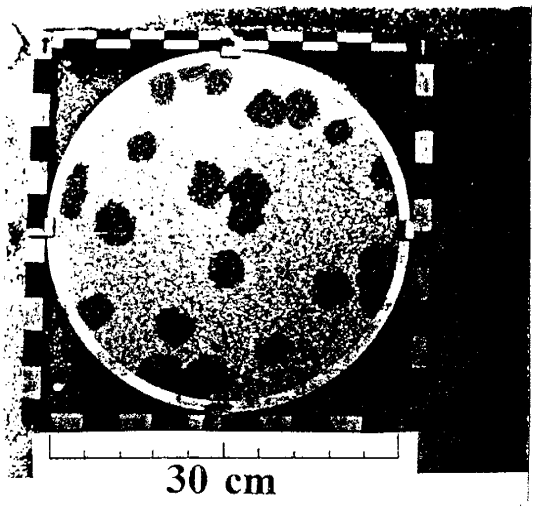

B. High Infiltration Rate (3.18 cm/hour)

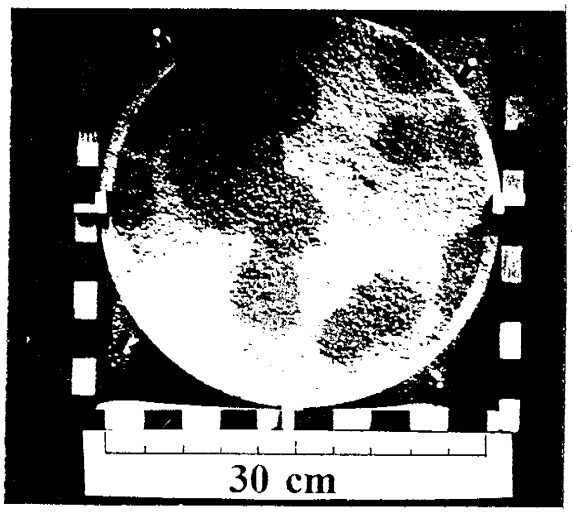

C. Low Infiltration Rate (0.138 cm/hour)

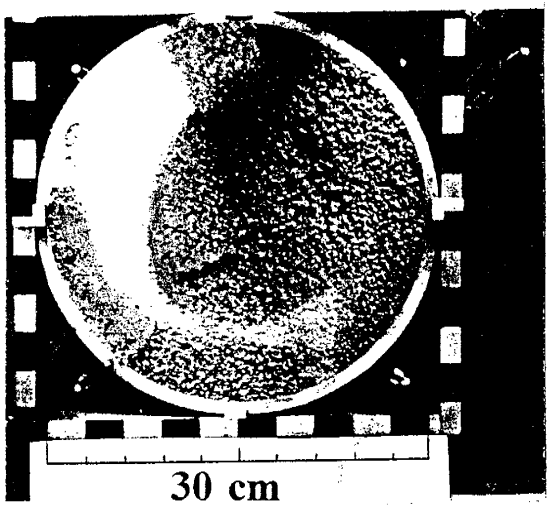

D. Low Infiltration Rate (0.12 cm/hour)

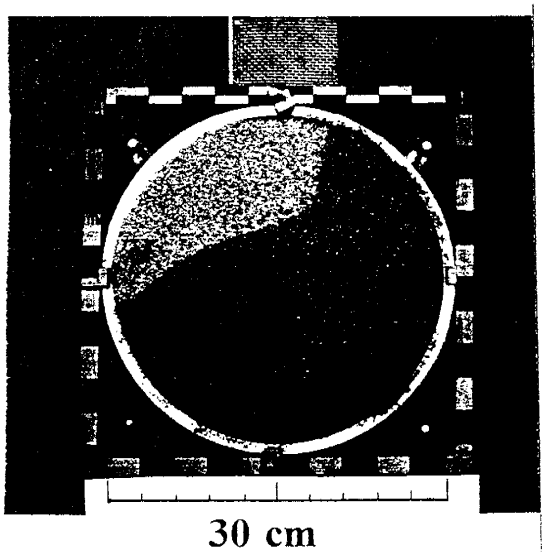

higher infiltration rates. The stable phenomena at very low infiltration rates have not been directly pointed out by any previous stability theories but may have been implied by some of them; for example, Glass et al. (1989b) reported that under low flow rates the fingers tend to have a meandering behavior. This property allows fingers to hit each other, resulting in larger fingers. But they still concluded that under the low infiltration rate, fingers should reach a minimum size and that Eq. (1) should be sustained under all conditions. Philip (1975a) addressed the fact that finger flow is gravity driven; where gravity plays no part, there is no mechanism to cause instability. The absence of gravity is basically the same as the condition necessary for horizontal absorption. Gravity has no effect on the flow or is insignificant to the absorption processes and capillary forces dominate the process. The surface tension which manifests itself through capillarity helps to stabilize the wetting front. Under these conditions the wetting front should always be stable. This phenomena is seen in the preliminary numerical experiments from the stability analysis of Stone and Hendrickx (1993) which uses the van Genuchten soil parameters.

Prediction of Finger Diameter

Table 3 shows the finger diameters predicted by eq. (1) using the measured parameters in Table 2. The predicted diameters increase when grain size becomes finer; sorptivity increases and saturated conductivity decreases. The deviating diameter of 3.6 cm in 40-60 cm sand is a result of the low sorptivity value (see Table 2) measured previously. In general, Eq. (1) is able to predict relative finger diameters quite well. However, the absolute accuracy may be off by a factor of 2. The lack of accuracy is

caused by the fact that the sorptivity of coarse sand is very hard to measure, especially in the region of the water-entry value. The high uncertainty of sorptivity measurements has been discussed before by Selker et al. (1992) and seems to be a major bottleneck to a more accurate prediction of finger diameters.

Table 3. Predictions and Observations of Finger Diameters.

Sand Size	Predicted Diameters†	Predicted Diameters‡	Observations (Range)
(US Mesh)	cm	cm	cm
14-20	1.56	1.56	3-6
20-30	7.70	4.18	4-7
30-40	12.48	6.90	6-11
40-60	3.60	9.97	10-18

† Using water entry values based on the Brooks and Corey equation.

‡ Using water entry values based on the capillary rise experiments.

CONCLUSION

Our experimental work demonstrates that wetting fronts in wettable and initially dry homogeneous soils tend to become stable at low water application rates. Therefore, the formula by Glass et al. (1989a,b) should not be used to predict finger diameters at low infiltration rates. Experimental results show that, when gravity dominates the flow process under higher infiltration rates, the finger diameters can be approximately predicted with equation (1).

REFERENCES

Ankney, M.D., T.C. Kaspar, and R. Horton. 1988. Design for an automated tension infiltrometer. Soil Sci. Soc. Am. J. 52:893-896.

Baker, R.S., and D. Hillel. 1990. Laboratory tests of a theory of fingering during infiltration into layered soils. Soil Sci. Soc. Am. J. 54:20-30.

Beven, K., and P. Germann. 1982. Macropores and water flow in soils. Water Resour. Res. 18(5):1311-1325.

Bouma, J. 1980. Soil morphology and preferential flow along macropores. Agri. Water Management. 3:235-250.

Bubenzer, G.D., 1979. Rainfall characteristics important for simulation. p. 22-34. *In* Proceedings of rainfall simulator workshop, Tucson, AZ. 7-9 Mar. 1979.

Carter, C.E., J.D. Greer, H.J. Braud, and J.M. Floyd. 1974. Raindrop characteristics in south central United States. Trans. ASAE. 17(6):1033-1037.

Diment, G. A., and K. K. Watson. 1983. Stability analysis of water movement in unsaturated porous materials: 2. Numerical studies. Water Resour. Res. 19:1002-1010.

Diment, G. A., and K. K. Watson. 1985. Stability analysis of water movement in unsaturated porous materials: 3. Experimental studies. Water Resour. Res. 21:979-984.

Diment, G. A., K. K. Watson, and P. J. Blennerhassett. 1982. Stability analysis of water movement in unsaturated porous materials: 1. Theoretical considerations. Water Resour. Res. 18:1248-1254.

Glass, R. J., J. King, S. Cann, N. Bailey, J.-Y. Parlange, and T. S. Steenhuis. 1990.

Wetting front instability in unsaturated porous media: A three-dimensional study. Transp. Porous Media. 5: 247-268.

Glass, R.J., J.-Y. Parlange., and T.S. Steenhuis, 1991. Immiscible displacement in porous media: Stability analysis of three-dimensional, axisymmetric disturbances with application to gravity-driven wetting front instability. Water Resour. Res. 27:1947-1956.

Glass, R.J., T.S. Steenhuis, and J.-Y. Parlange. 1989a. Wetting front instability: 1. Theoretical discussion and dimensional analysis. Water Resour. Res. 25:1187-1194.

Glass, R.J., T.S. Steenhuis, and J.-Y. Parlange. 1989b. Wetting front instability: 2. Experimental determination of relationships between system parameters and two-dimensional unstable flow field behavior in initially dry porous media. Water Resour. Res. 25:1195-1207.

Glass, R.J., T.S. Steenhuis, and J.-Y. Parlange. 1989c. Mechanism for finger persistence in homogeneous, unsaturated, porous media: theory and verification. Soil Sci. 148:60-70.

Hagerman, J.R., N.B. Pickering, W.F. Ritter, and T.S. Steenhuis. 1989. In situ measurement of preferential flow. ASCE National Water Conference and Symposium, Newark, Delaware. pp. 10.

Hendrickx, J.M.H., and L.W. Dekker. 1991. Experimental evidence of unstable wetting fronts in non-layered soils. p. 22-31. *In* Proc. Natl. Symp. Preferential Flow, Chicago,IL. 16-17 Dec. 1991. Am. Soc. Agric. Eng., St. Joseph, MI.

Hendrickx, J.M.H., L.W. Dekker, and O.H. Boersma. 1993. Unstable wetting fronts in water repellent field soils. J. of Environmental Quality. 22:109-118.

Hendrickx, J.M.H., L.W. Dekker, and P.A.C. Raats. 1988a. Formation of sand columns caused by unstable wetting fronts. Grondboor en Hamer. 6:173-175. (in Dutch).

Hendrickx, J.M.H., L.W. Dekker, E.J. Van Zuilen, and O.H. Boersma. 1988b. Water and solute movement through a water repellent sand soil with grass cover. pp. 131-146. *In* Wierenga, P.J. and D. Bachelet. Validation of flow and transport models for the unsaturated zone: Conference Proceedings; May 23-26, 1988 Ruidoso, New Mexico. Research Report 88-SS-04 Dept. of Agronomy and Horticulture, New Mexico State University, Las Cruces, N.M. 545 p.

Hill, D.E., and J.-Y. Parlange. 1972. Wetting front instability in layered soils. Soil Sci. Soc. Am. Proc. 36:697-702.

Hillel, D., and R.S. Baker. 1988. A descriptive theory of fingering during infiltration into layered soils. Soil Sci. 146:51-56.

Laws, J.O., and D.A. Parsons. 1943. Relation of raindrop size to intensity. Trans. Am. Geophy. Union. 24:452-460.

Parlange, J.-Y., and D.E. Hill. 1976. Theoretical analysis of wetting front instability in soils. Soil Sci. 122:236-239.

Philip, J.R. 1975a. Stability analysis of infiltration. Soil Sci. Soc. Am. Proc. 39:1042-1049.

Philip, J.R. 1975b. The growth of disturbances in unstable infiltration flows. Soil Sci. Soc. Am. Proc. 39 :1049-1053.

Raats, P.A.C. 1973. Unstable wetting fronts in uniform and nonuniform soils. Soil Sci. Soc. Am. Proc. 37:681-685.

Ritsema, C.J., L.W. Dekker, J.M.H. Hendrickx, and W. Hamminga. 1993. Preferential flow mechanism in a water-repellent sandy soil. Water Resour. Res. 29:2183-2193.

Saffman, P.G. 1986. Viscous fingering in Hele Shaw cells. J. Fluid Mech. 173:73.

Selker, J.S., T.S. Steenhuis, and J.-Y. Parlange. 1989. Preferential flow in homogeneous sandy soils without layering. Paper No. 89-2543, Am. Soc. Agric. Eng., Winter Meeting, New Orleans. p. 22.

Selker, J.S., T.S. Steenhuis, and J.-Y. Parlange. 1992. Wetting front instability in homogeneous sandy soils under continuous infiltration. Soil Sci. Soc. Am. J. 56:1346-1350.

Stone W.D., and J.M.H. Hendrickx. 1993. Stability of wetting fronts in van Genuchten soils. p. 149. *In* 1993 Spring Meeting. Am. Geophy. Union. Baltimore, MA. 24-28 May. 1993.

Tabuchi, T. 1961. Infiltration and ensuing percolation in columns of layered glass particles packed in laboratory (In Japanese, with a summary in English). Nogyo dobuku kenkyn, Bessatsu (Trans. Agr. Eng. Soc., Japan). 1:13-19.

Tamai, N., T. Asaeda, and C.G. Jeevaraj. 1987. Fingering in two-dimensional, homogeneous, unsaturated porous media. Soil Sci. 144:107-112.

van Genuchten, M.Th., F. J. Leij, and S. R. Yates. 1991. The RETC code for quantifying the hydraulic functions of unsaturated soils. U.S. Salinity Laboratory, U. S. Department of Agriculture, Agricultural Research Service, Riverside, CA.

Van Ommen, H.C., R. Dijksma, J.M.H. Hendrickx, L.W. Dekker, J. Hulshof, and

M. van den Heuvel. 1989. Experimental assessment of preferential flow paths in a field soil. J. of Hydrology 105:253-262.

White, I., P.M. Colombera, and J.R. Philip. 1976. Experimental study of wetting front instability induced by sudden change of pressure gradient. Soil Sci. Soc. Am. J. 40:824-829.

Yao, T., and J.M.H. Hendrickx. 1993. A laboratory study of wetting front stability. p. 150. *In* 1993 Spring Meeting. Am. Geophy. Union. Baltimore, MA. 24-28 May. 1993.

APPENDIX A

WATER RETENTION CURVE MEASUREMENTS OF PERLITE SAND

APPENDIX A

WATER RETENTION CURVE MEASUREMENTS OF PERLITE SAND

This appendix contains the water retention curves and van Genuchten parameters of our experimental material: perlite sand.

For each of the grades we determined the water retention curves with the hanging water column technique on 100 cm^3 dry samples that were taken in-situ from the lysimeters. The porous plate was pre-saturated and the bottom part was filled with distilled water; this device was then taken to connect to the buret set which was pre-filled with distilled water to the top reading of the buret. After taking the first water level reading from the buret, we put the totally dry sample on the top of the porous plate. The height of the sample was fixed. By gradually moving the buret from the low position to the sample position, the wetting curve was obtained. For our sand, the position of the buret started at 120 cm below the sample position (which is the average height of the sample ring). The buret was moved up 3-5 cm each time, then allowed 4-6 hours to let it reach equilibrium. The buret reading and the height of the water table inside the buret were both taken. Since the soil sample started at zero water content, the decreased amount of water in the buret was absorbed by the soil. This amount is equal to the water content of the sample. The head difference between the sample and the water table inside the buret represents the tension of the soil. By plotting the water content versus tension, the wetting curve was then obtained. In the same manner, when we moved the buret down from the height of the sample gradually, the drying curve could determined. The van Genuchten soil parameters were obtained by fitting the water retention data through the

RETC curve fitting computer program.

The RETC (RETention Curve) computer code was written for the purpose of analyzing the soil water retention and hydraulic conductivity functions of unsaturated soils. The program uses the parametric models of Brooks-Corey and van Genuchten to represent the soil water retention curve, and the theoretical pore-size distribution models of Mualem and Burdine to predict the unsaturated hydraulic conductivity function from observed soil water retention data. In this appendix, water retention data were fit by the V-G equation. As stated in Appendix D, the water entry-value was obtained by fitting data with the Brooks-Corey equation. These two equations are listed as below:

van-Genuchten equation

$$\frac{\theta-\theta_r}{\theta_s-\theta_r}=\frac{1}{[1+(\alpha h)^n]^m} \quad \ldots\ldots\ldots Eq.\ (A\text{-}1)$$

where α n, m, θ_s ,and θ_r are fitting parameters (θ_s is saturated water content and θ_r is residual water content; both can be set as constant) and θ (water content inside the soil sample) and h (tension inside the soil sample) are from the water retention data. The values of α n, and m are empirical parameters that describe the shape of the water retention curve.

Brooks-Corey equation

$$\theta=\begin{cases}\theta_r+(\theta_s-\theta_r)\ (\alpha h)^{-\lambda} \ldots\ldots (\alpha h>1)\\ \theta_s \ldots\ldots\ldots\ldots\ldots\ldots (\alpha h\le 1)\end{cases} \quad \ldots\ldots\ldots Eq.\ (A\text{-}2)$$

where α is an empirical parameter (L^{-1}) whose inverse is often referred to as the air-entry value for the wetting curve and as the water-entry value for the drying curve. λ is

a pore-size distribution parameter affecting the slope of the retention function. The nonlinear least-squares parameter optimization method is used for estimating the unknown coefficients.

Figures A-1 through A-4 show the water retention curves of our four grades of perlite sand. Table A-1 shows the van genuchten parameters for both the wetting and dying curves. The fitted curves are also shown in Figs. A-1 through A-4.

Fig. A-1. 14-20 Sand Water Retention Curve

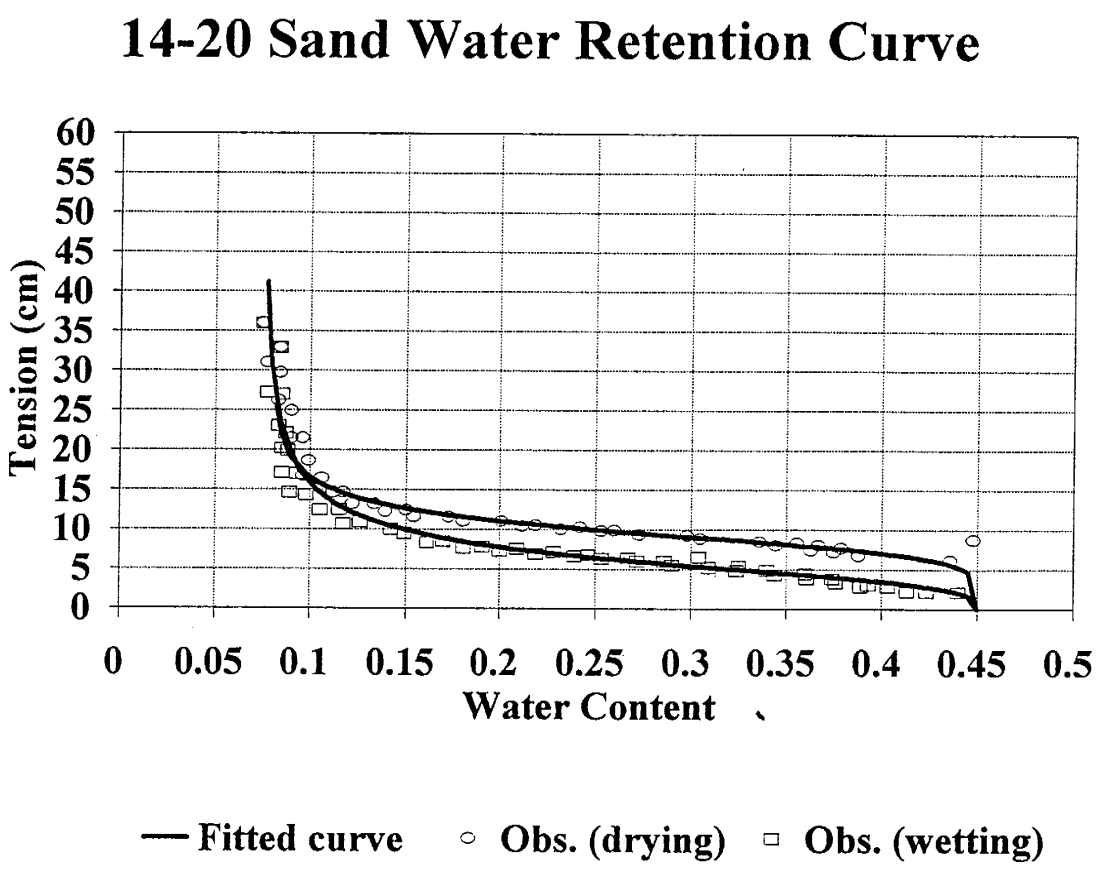

Fig. A-2. 20-30 Sand Water Retention Curve

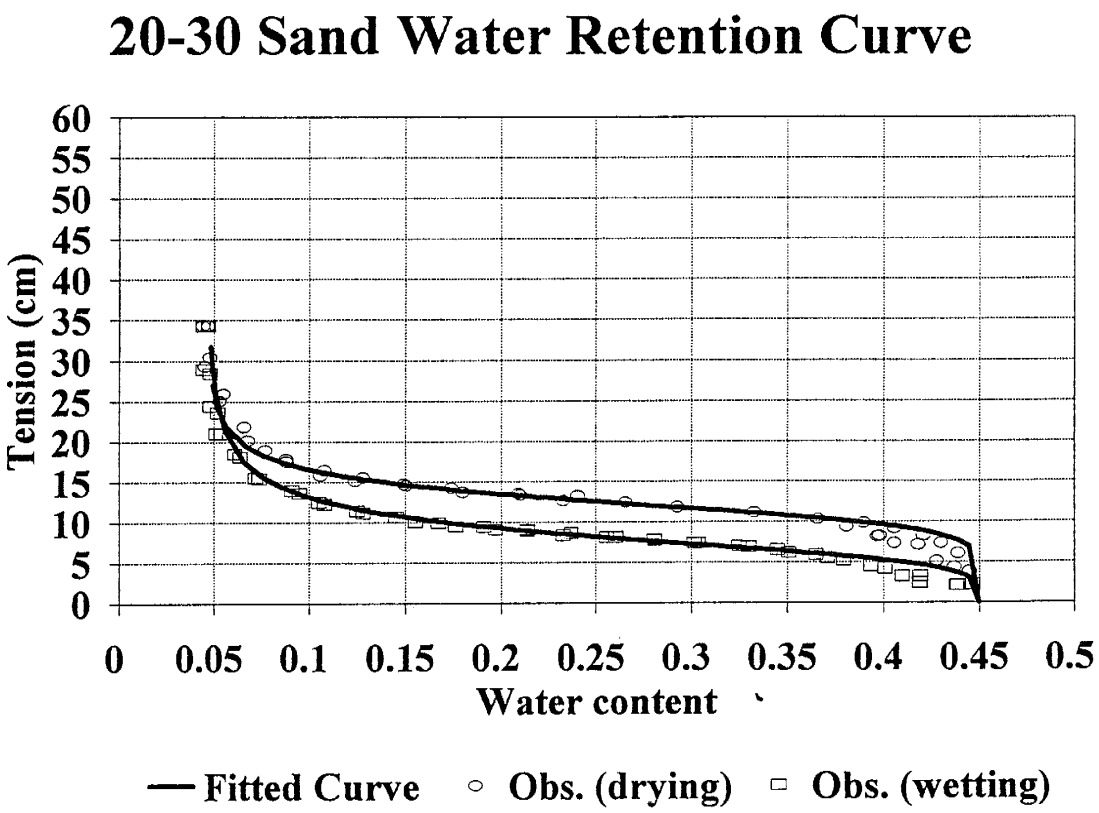

Fig. A-3. 30-40 Sand Water Retention Curve

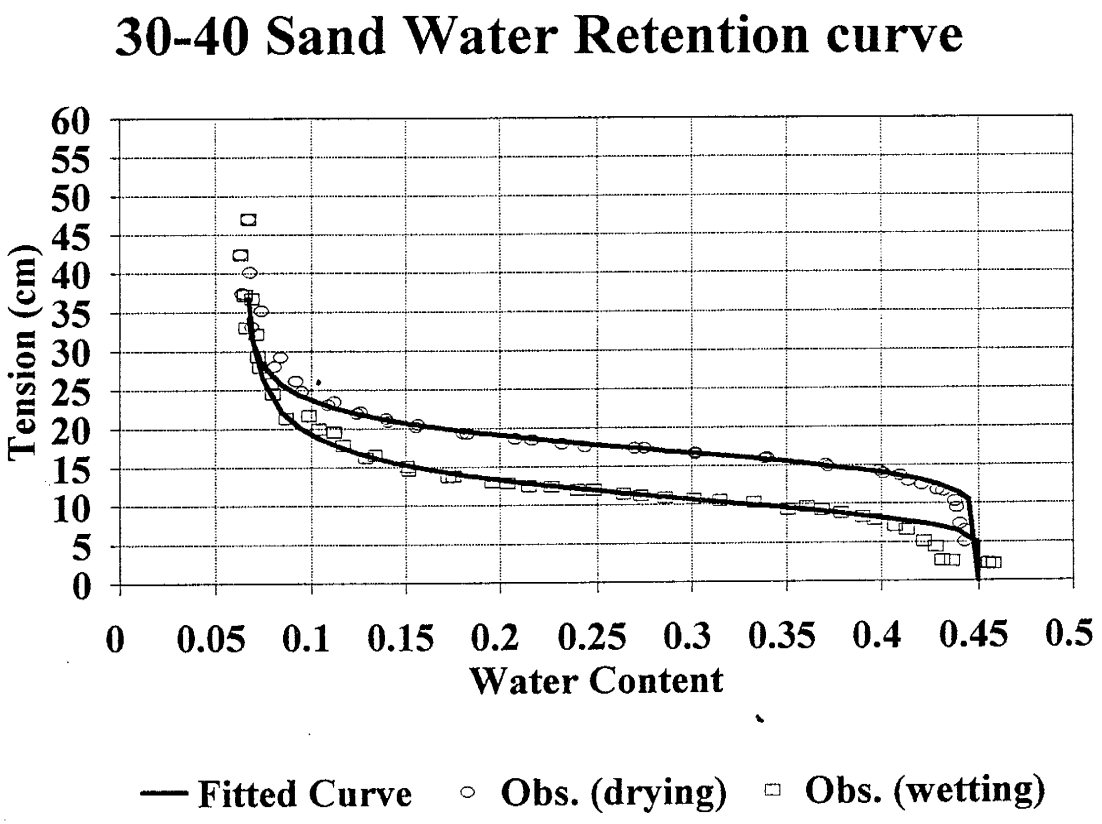

Fig. A-4. 40-60 Sand Water Retention Curve

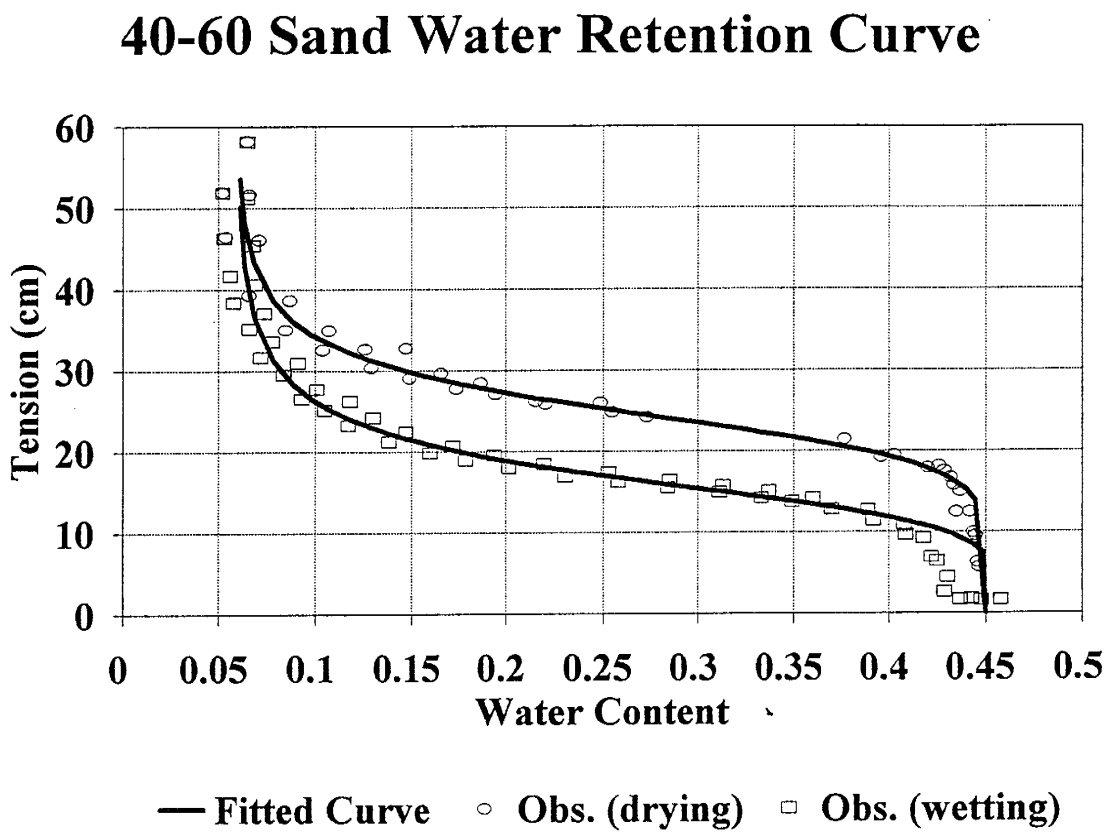

Table A-1. Fitted Parameters of Perlite Sand.

Grade (U.S. Sieve)	θ_s (-)	θ_r (-)	α (L^{-1})	n (-)	r^2
14-20(drying)	.45	.075	.108	6.020	.990
14-20(wetting)			.188	3.480	.983
20-30(drying)	.45	.044	.083	6.537	.994
20-30(wetting)			.131	4.499	.994
30-40(drying)	.45	.063	.058	8.305	.998
30-40(wetting)			.092	5.068	.995
40-60(drying)	.45	.052	.041	7.240	.994
40-60(wetting)			.062	5.186	.991

APPENDIX B

LYSIMETER EXPERIMENTS SUMMARY

APPENDIX B

LYSIMETER EXPERIMENTS SUMMARY

The patterns of the fingers in our lysimeter experiments were photographed. These photographs were used to determine the finger diameter, the wetting area ratio and the distance between the fingers. The image process software Khoros (from UNM) was supposed to have been used to analyze these photographs, but some technical problems have not yet been solved. Only the visual measurements of the finger sizes and some of the wetting area ratio (measured by points counting and a planimeter) are available at this time.

For our experiments there are several parameters we kept as variables, such as water application rates, the total amount of application, and the sand sizes. The top layers were kept completely wet throughout our experiments. Dry spots usually appeared within a depth of 10 cm. For most of our 40-60 sand the dry spots started at a depth of around 10 cm or even deeper.

The following experimental results include summary tables and photographs. In the summary tables, the experimental conditions, experimental equipment, and a brief summary of results are shown. Table B-1 shows the results of the small lysimeter experiments. Table B-2 shows the results from the large lysimeter. Figures B-1(a-h), B-2 (a-j), and B-3 (a-f) show the large lysimeter experimental results of 14-20, 30-40, and 40-60 sand respectively.

For the water application, three different rainfall simulators were used. They were: (1) The hand sprayer, which was the equipment we initially used to approach high flow rates. (2)The disk sprinkler system, which was good for the low water application rates. (3) The oscillating sprinkler system, which was designed and built for our experiments. The design and the test results of the sprinkler systems are discussed further in Appendix E.

Table B-1. Small Lysimeter Experimental Results.

Small Lysimeter Experimental Results

Size	Date	Rate	Sprinkler Type	Total Amount	Depth	Finger Size	Wet Area
(US Mesh)		(cm/hour)		(cm)	(cm)	(cm)	(%)
14-20	09/06/91	7.98	h	6	10	0	92.7
14-20	09/06/91	7.98	h	6	20	0	82.5
14-20	09/06/91	7.98	h	6	30	4.83	50.3
14-20	09/06/91	7.98	h	6	40	4.25	41.4
14-20	09/13/91	0.258	s	6.4	30	0	97.5
14-20	09/13/91	0.258	s	6.4	40	0	71.3
14-20	09/19/91	12.6	h	4	10	0	18.2
14-20	09/19/91	12.6	h	4	20	0	17.5
14-20	09/19/91	12.6	h	4	30	0	22.6
14-20	09/19/91	12.6	h	4	40	3.36	22.3
14-20	09/19/91	12.6	h	4	50	0	19.7
14-20	09/23/91	0.138	s	5	30	0	72.3
14-20	09/23/91	0.138	s	5	40	13	42.4
14-20	09/26/91	3.18	h	4	10	0	76.1
14-20	09/26/91	3.18	h	4	20	4	38.5
14-20	09/26/91	3.18	h	4	30	0	34.1
14-20	09/26/91	3.18	h	4	40	4.2	20.7
14-20	09/30/91	0.129	s	4	20	0	90.4
14-20	09/30/91	0.129	s	4	30	0	53.8
14-20	09/30/91	0.129	s	4	40	0	8.3
14-20	10/03/91	1.602	h	4	10	0	95.5
14-20	10/03/91	1.602	h	4	20	0	79
14-20	10/03/91	1.602	h	4	30	0	47.1
14-20	10/03/91	1.602	h	4	40	0	48.7
14-20	10/07/91	0.498	s	2.5	10	5.3	43.6
14-20	10/07/91	0.498	s	2.5	20	6.15	36.3
14-20	10/07/91	0.498	s	2.5	30	0	5.1
14-20	10/15/91	1.41	s	4	10	0	70.7
14-20	10/15/91	1.41	s	4	20	4.5	32.8
14-20	10/15/91	1.41	s	4	30	4.5	27.4
14-20	10/15/91	1.41	s	4	40	5.75	25.2
14-20	10/17/91	1.41	s	4	10	4	36.6
14-20	10/17/91	1.41	s	4	20	4.5	28.7
14-20	10/17/91	1.41	s	4	30	4.75	27.4
14-20	10/17/91	1.41	s	4	40	4.5	20.7
20-30	09/06/91	7.98	h	6	10	0	99.5

Small Lysimeter Experimental Results

Size	Date	Rate	Sprinkler Type	Total Amount	Depth	Finger Size	Wet Area
(US Mesh)		(cm/hour)		(cm)	(cm)	(cm)	(%)
20-30	09/06/91	7.98	h	6	20	0	95.9
20-30	09/06/91	7.98	h	6	30	0	88.9
20-30	09/13/91	0.258	s	6.4	30	0	99.7
20-30	09/13/91	0.258	s	6.4	40	0	51
20-30	09/19/91	12.6	h	4	10	0	80.2
20-30	09/19/91	12.6	h	4	20	0	58.3
20-30	09/19/91	12.6	h	4	30	0	46.5
20-30	09/19/91	12.6	h	4	40	4.61	30.9
20-30	09/19/91	12.6	h	4	50	0	25.8
20-30	09/23/91	0.138	s	5	20	0	88.5
20-30	09/23/91	0.138	s	5	30	0	75.5
20-30	09/23/91	0.138	s	5	40	16	34.1
20-30	09/26/91	3.18	h	4	10	0	98.7
20-30	09/26/91	3.18	h	4	20	0	71.7
20-30	09/26/91	3.18	h	4	30	6.5	39.8
20-30	09/26/91	3.18	h	4	40	7.75	20.4
20-30	09/30/91	0.129	s	4	20	0	94.3
20-30	09/30/91	0.129	s	4	30	0	10.2
20-30	09/30/91	0.129	s	4	40	0	0
20-30	10/03/91	1.602	h	4	20	0	78.3
20-30	10/03/91	1.602	h	4	30	5.46	39.8
20-30	10/03/91	1.602	h	4	40	5.8	12.7
20-30	10/07/91	0.498	s	2.5	10	0	47.8
20-30	10/07/91	0.498	s	2.5	20	10	35
20-30	10/07/91	0.498	s	2.5	30	0	8.9
20-30	10/15/91	1.41	s	4	10	0	93.6
20-30	10/15/91	1.41	s	4	20	0	48.4
20-30	10/15/91	1.41	s	4	30	0	39.8
20-30	10/15/91	1.41	s	4	40	5.5	25.8
20-30	10/17/91	1.41	s	4	10	0	63.4
20-30	10/17/91	1.41	s	4	20	0	16.6
20-30	10/17/91	1.41	s	4	30	0	12.7
20-30	10/17/91	1.41	s	4	40	4.5	20.4
30-40	09/06/91	5.88	h	6	30	0	95.2
30-40	09/06/91	5.88	h	6	40	0	62.7
30-40	09/13/91	0.258	s	6.4	30	0	99.7

Small Lysimeter Experimental Results

Size	Date	Rate	Sprinkler Type	Total Amount	Depth	Finger Size	Wet Area
(US Mesh)		(cm/hour)		(cm)	(cm)	(cm)	(%)
30-40	09/13/91	0.258	s	6.4	40	0	49
30-40	09/19/91	12.6	h	4	10	0	65.9
30-40	09/19/91	12.6	h	4	20	0	45.2
30-40	09/19/91	12.6	h	4	30	7	15.3
30-40	09/19/91	12.6	h	4	40	0	10.2
30-40	09/19/91	12.6	h	4	50	0	20.1
30-40	09/23/91	0.138	s	5	30	0	57.3
30-40	09/23/91	0.138	s	5	40	0	88.2
30-40	09/26/91	3.18	h	4	10	0	82.8
30-40	09/26/91	3.18	h	4	20	7.63	53.5
30-40	09/26/91	3.18	h	4	30	0	40.1
30-40	09/26/91	3.18	h	4	40	0	24.2
30-40	09/30/91	0.129	s	4	50	0	81.8
30-40	09/30/91	0.129	s	4	30	0	13.4
30-40	09/30/91	0.129	s	4	40	0	0
30-40	10/03/91	1.602	h	4	20	0	68.2
30-40	10/03/91	1.602	h	4	30	0	42.7
30-40	10/03/91	1.602	h	4	40	0	6.4
30-40	10/07/91	0.498	s	2.5	10	0	36
30-40	10/07/91	0.498	s	2.5	20	0	9.6
30-40	10/07/91	0.498	s	2.5	30	0	16.9
30-40	10/07/91	0.498	s	2.5	40	0	17.2
30-40	10/15/91	1.41	s	4	10	0	55.4
30-40	10/15/91	1.41	s	4	20	0	26.8
30-40	10/17/91	2.76	s	4	10	0	83.4
40-60	09/06/91	5.88	h	6	20	0	96.5
40-60	09/06/91	5.88	h	6	30	0	69.1
40-60	09/06/91	5.88	h	6	40	0	71
40-60	09/13/91	0.258	s	6.4	30	0	95.5
40-60	09/13/91	0.258	s	6.4	40	0	84.1
40-60	09/19/91	15	h	4	10	0	81.2
40-60	09/26/91	3.18	h	5	10	0	75.8
40-60	09/26/91	3.18	h	5	20	0	44.6
40-60	09/30/91	0.129	s	4	30	0	59.2
40-60	09/30/91	0.129	s	4	40	0	0
40-60	10/03/91	1.602	h	4	20	0	89.5

Small Lysimeter Experimental Results

Size	Date	Rate	Sprinkler Type	Total Amount	Depth	Finger Size	Wet Area
(US Mesh)		(cm/hour)		(cm)	(cm)	(cm)	(%)
40-60	10/03/91	1.602	h	4	30	0	8
40-60	10/03/91	1.602	h	4	40	0	1.3
40-60	10/07/91	0.498	s	2.5	10	0	70.1
40-60	10/07/91	0.498	s	2.5	20	0	2.5
40-60	10/15/91	1.41	s	4	10	0	82.2
40-60	10/17/91	2.76	s	4	10	0	80.3
14-20	10/21/91	4.14	s	4	10	0	75.8
14-20	10/21/91	4.14	s	4	20	0	44.2
14-20	10/21/91	4.14	s	4	30	0	27.7
14-20	10/21/91	4.14	s	4	40	5.2	27.1
14-20	10/21/91	4.14	s	4	10	0	55.7
14-20	10/21/91	4.14	s	4	20	0	36.9
14-20	10/21/91	4.14	s	4	30	7.7	45.5
14-20	10/21/91	4.14	s	4	40	0	39.5
14-20	10/21/91	4.14	s	4	10	0	68.8
14-20	10/21/91	4.14	s	4	20	0	45.2
14-20	10/21/91	4.14	s	4	30	0	35.7
14-20	10/21/91	4.14	s	4	40	0	32.5
14-20	10/21/91	4.14	s	4	10	0	87.9
14-20	10/21/91	4.14	s	4	20	0	54.1
14-20	10/21/91	4.14	s	4	30	0	51.2
14-20	10/21/91	4.14	s	4	40	0	51.9
14-20	10/27/91	6.858	s	4	20	0	96.8
14-20	10/27/91	6.858	s	4	30	0	94.6
14-20	10/27/91	6.858	s	4	40	0	68.2
14-20	10/27/91	6.858	s	4	10	0	99
14-20	10/27/91	6.858	s	4	20	0	35
14-20	10/27/91	6.858	s	4	30	0	29.9
14-20	10/27/91	6.858	s	4	40	0	44.6
14-20	10/27/91	6.858	s	4	10	0	70.7
14-20	10/27/91	6.858	s	4	20	0	50.9
14-20	10/27/91	6.858	s	4	30	0	37.6
14-20	03/10/92	6.858	s	4	10	0	57.9
14-20	03/10/92	6.858	s	4	20	5.2	41.7
14-20	03/10/92	6.858	s	4	30	4.9	26.1
14-20	03/10/92	6.858	s	4	40	4.8	33.1

Small Lysimeter Experimental Results

Size	Date	Rate	Sprinkler Type	Total Amount	Depth	Finger Size	Wet Area
(US Mesh)		(cm/hour)		(cm)	(cm)	(cm)	(%)
14-20	03/10/92	6.858	s	4	10	0	58.9
14-20	03/10/92	6.858	s	4	20	4.8	46.5
14-20	03/10/92	6.858	s	4	30	5.6	29.3
14-20	03/10/92	6.858	s	4	40	5.75	38.2
14-20	03/10/92	6.858	s	4	10	0	66.9
14-20	03/10/92	6.858	s	4	20	5.5	50.9
14-20	03/10/92	6.858	s	4	30	5.4	50.9
14-20	03/10/92	6.858	s	4	40	5.6	43.3
14-20	03/10/92	6.858	s	4	10	0	75.8
14-20	03/10/92	6.858	s	4	20	0	50.9
14-20	03/10/92	6.858	s	4	30	5.75	42.7
14-20	03/10/92	6.858	s	4	40	6	46.2
14-20	03/19/92	6.858	s	4	10	0	59.2
14-20	03/19/92	6.858	s	4	20	4	44.9
14-20	03/19/92	6.858	s	4	30	4.4	39.8
14-20	03/19/92	6.858	s	4	40	5	74.2
14-20	03/19/92	6.858	s	4	10	0	57.3
14-20	03/19/92	6.858	s	4	20	0	42.7
14-20	03/19/92	6.858	s	4	30	4.6	29.3
14-20	03/19/92	6.858	s	4	40	0	45.8
14-20	03/19/92	6.858	s	4	10	0	62.1
14-20	03/19/92	6.858	s	4	20	5.1	42
14-20	03/19/92	6.858	s	4	30	5.8	34.1
14-20	03/19/92	6.858	s	4	40	0	74.5
14-20	03/19/92	6.858	s	4	10	0	77.7
14-20	03/19/92	6.858	s	4	20	5.9	46.8
14-20	03/19/92	6.858	s	4	30	6.1	35
14-20	03/19/92	6.858	s	4	40	0	72.3
14-20	03/26/92	5.22	s	4	10	0	69.1
14-20	03/26/92	5.22	s	4	20	5.1	50.3
14-20	03/26/92	5.22	s	4	30	5	45.2
14-20	03/26/92	5.22	s	4	40	5.4	45.2
20-30	03/26/92	5.22	s	4	10	0	79.6
20-30	03/26/92	5.22	s	4	20	5.3	47.7
20-30	03/26/92	5.22	s	4	30	6.1	54.4
20-30	03/26/92	5.22	s	4	40	5.2	67.2

Small Lysimeter Experimental Results

Size	Date	Rate	Sprinkler Type	Total Amount	Depth	Finger Size	Wet Area
(US Mesh)		(cm/hour)		(cm)	(cm)	(cm)	(%)
14-20	03/26/92	5.22	s	4	10	0	67.5
14-20	03/26/92	5.22	s	4	20	4.8	45.2
14-20	03/26/92	5.22	s	4	30	4.3	46.5
14-20	03/26/92	5.22	s	4	40	0	47.4
14-20	03/26/92	5.22	s	4	10	0	89.5
14-20	03/26/92	5.22	s	4	20	0	62.1
14-20	03/26/92	5.22	s	4	30	0	62.8
14-20	03/26/92	5.22	s	4	40	0	58.9
20-30	04/29/92	4.284	s	4	10	0	75.2
20-30	04/29/92	4.284	s	4	20	6.7	47.1
20-30	04/29/92	4.284	s	4	30	6.8	31.5
20-30	04/29/92	4.284	s	4	10	4.68	33.8
20-30	04/29/92	4.284	s	4	20	4.63	32.3
20-30	04/29/92	4.284	s	4	30	4.5	42.9
20-30	04/29/92	4.284	s	4	40	4.5	27.2
20-30	04/29/92	4.284	s	4	10	4.87	60.2
20-30	04/29/92	4.284	s	4	20	5.08	46.5
20-30	04/29/92	4.284	s	4	30	4	35.4
20-30	04/29/92	4.284	s	4	40	4	27.2
20-30	04/29/92	4.284	s	4	10	6	76.8
20-30	04/29/92	4.284	s	4	20	6.08	50.9
20-30	04/29/92	4.284	s	4	30	5.85	48.7
20-30	04/29/92	4.284	s	4	40	8	39
14-20	09/22/92	8.88	os	4	10	3	N.A
14-20	09/22/92	8.88	os	4	20	3.2	N.A
14-20	09/22/92	8.88	os	4	30	3.1	21.9
14-20	09/22/92	8.88	os	4	40	3.6	N.A
14-20	09/29/92	9.06	os	2	10	2.61	N.A
14-20	09/29/92	9.06	os	2	20	2.77	N.A
14-20	09/29/92	9.06	os	2	30	2.75	N.A
14-20	09/29/92	9.06	os	2	40	2.9	N.A
14-20	09/29/92	9.06	os	4	10	3.9	N.A
14-20	09/29/92	9.06	os	4	20	3	N.A
14-20	09/29/92	9.06	os	4	30	3	N.A
14-20	09/29/92	9.06	os	4	40	2.9	N.A
14-20	09/29/92	9.06	os	6	10	0	N.A

Small Lysimeter Experimental Results

Size	Date	Rate	Sprinkler Type	Total Amount	Depth	Finger Size	Wet Area
(US Mesh)		(cm/hour)		(cm)	(cm)	(cm)	(%)
14-20	09/29/92	9.06	os	6	20	5.65	N.A
14-20	09/29/92	9.06	os	6	30	5.5	29.3
14-20	09/29/92	9.06	os	6	40	7	N.A
14-20	09/29/92	9.06	os	6	10	3.23	N.A
14-20	09/29/92	9.06	os	6	20	3.96	N.A
14-20	09/29/92	9.06	os	6	30	3.33	N.A
14-20	09/29/92	9.06	os	6	40	4.1	N.A
14-20	10/09/92	9.06	os	6	10	3.32	N.A
14-20	10/09/92	9.06	os	6	20	3.62	N.A
14-20	10/09/92	9.06	os	6	30	3.52	25.3
14-20	10/09/92	9.06	os	6	40	3.46	N.A
14-20	10/09/92	9.06	os	8	10	3.49	N.A
14-20	10/09/92	9.06	os	8	20	3.66	N.A
14-20	10/09/92	9.06	os	8	30	3.52	N.A
14-20	10/09/92	9.06	os	8	40	0	N.A
14-20	10/20/92	9.06	os	4	10	0	N.A
14-20	10/20/92	9.06	os	4	20	3.03	N.A
14-20	10/20/92	9.06	os	4	30	3	N.A
14-20	10/20/92	9.06	os	4	40	0	N.A
14-20	10/20/92	3	os	4	10	3.27	N.A
14-20	10/20/92	3	os	4	20	3.64	N.A
14-20	10/20/92	3	os	4	30	3.72	31.3
14-20	10/20/92	3	os	4	40	3.4	N.A
20-30	11/20/92	266.64	os	4	10	4.9	N.A
20-30	11/20/92	266.64	os	4	20	5.1	N.A
20-30	11/20/92	266.64	os	4	30	5	21.5
20-30	11/20/92	266.64	os	4	40	5.3	N.A
40-60	04/20/93	26.1	os	4	10	0	N.A
40-60	04/20/93	26.1	os	4	20	11.5	N.A
40-60	04/20/93	26.1	os	4	30	9.5	8
40-60	04/20/93	26.1	os	4	40	10.5	N.A
30-40	04/20/93	26.1	os	4	10	5.43	N.A
30-40	04/20/93	26.1	os	4	20	5.33	N.A
30-40	04/20/93	26.1	os	4	30	5.67	N.A
30-40	04/20/93	26.1	os	4	40	5	N.A
14-20	03/02/93	0.12	os	4	10	0	N.A

Small Lysimeter Experimental Results

Size	Date	Rate	Sprinkler Type	Total Amount	Depth	Finger Size	Wet Area
(US Mesh)		(cm/hour)		(cm)	(cm)	(cm)	(%)
14-20	03/02/93	0.12	os	4	20	0	N.A
14-20	03/02/93	0.12	os	4	30	0	N.A
14-20	03/02/93	0.12	os	4	40	0	N.A
14-20	02/25/93	0.1482	os	4	10	0	N.A
14-20	02/25/93	0.1482	os	4	20	0	N.A
14-20	02/25/93	0.1482	os	4	30	0	0
14-20	02/25/93	0.1482	os	4	40	0	0
40-60	02/25/93	12.96	os	4	10	0	N.A
40-60	02/25/93	12.96	os	4	20	17.5	N.A
40-60	02/25/93	12.96	os	4	30	0	0
40-60	02/25/93	12.96	os	4	40	0	0
20-30	04/29/93	0.258	os	4	10	0	100
20-30	04/29/93	0.258	os	4	20	0	N.A
20-30	04/29/93	0.258	os	4	30	0	N.A
20-30	04/29/93	0.258	os	4	40	0	0
30-40	04/30/93	0.72	os	4	10	0	100
30-40	04/30/93	0.72	os	4	20	8	N.A
30-40	04/30/93	0.72	os	4	30	0	0
30-40	04/30/93	0.72	os	4	40	0	0
30-40	04/30/93	0.276	os	4	10	0	100
30-40	04/30/93	0.276	os	4	20	0	2
30-40	04/30/93	0.276	os	4	30	0	0
30-40	04/30/93	0.276	os	4	40	0	0
40-60	04/29/93	1.602	os	4	10	0	100
40-60	04/29/93	1.602	os	4	20	11.5	N.A
40-60	04/29/93	1.602	os	4	30	10	N.A
40-60	04/29/93	1.602	os	4	40	10	N.A

For sprinkler system
h: hand sprayer
s: disk sprinkler system
os: oscillating sprinkler system

Table B-2. Large Lysimetre Experimental Results.

Large Lysimeter Experimental Results

Size	Date	Rate	Sprinkler Type	Total Amount	Depth	Finger Size
(US Mesh)		(cm/hour)		(cm)	(cm)	(cm)
14-20	11/20/91	4.02	s	4	7.5	4.5
14-20	11/20/91	4.02	s	4	15	3.7
14-20	11/20/91	4.02	s	4	22.5	4.8
14-20	11/20/91	4.02	s	4	30	5.6
14-20	11/20/91	4.02	s	4	37.5	6.2
14-20	11/20/91	4.02	s	4	45	7.5
14-20	11/20/91	4.02	s	4	52.5	5.55
14-20	11/20/91	4.02	s	4	60	7.5
30-40	12/19/91	6.36	s	4	7.5	N.A.
30-40	12/19/91	6.36	s	4	15	N.A.
30-40	12/19/91	6.36	s	4	22.5	12.3
30-40	12/19/91	6.36	s	4	30	10.5
30-40	12/19/91	6.36	s	4	37.5	13
30-40	12/19/91	6.36	s	4	45	N.A.
40-60	02/20/92	6	s	4	7.5	N.A.
40-60	02/20/92	6	s	4	15	N.A.
40-60	02/20/92	6	s	4	22.5	N.A.
40-60	02/20/92	6	s	4	30	34
40-60	02/20/92	6	s	4	37.5	34
30-40	11/24/92	9	os	4	7.5	N.A.
30-40	11/24/92	9	os	4	15	7.4
30-40	11/24/92	9	os	4	22.5	7.2
30-40	11/24/92	9	os	4	30	8.6
30-40	11/24/92	9	os	4	37.5	9.6
30-40	11/24/92	9	os	4	45	11.76
30-40	11/24/92	9	os	4	52.5	13.1
30-40	11/24/92	9	os	4	60	11.67
30-40	11/24/92	9	os	4	67.5	10.83
30-40	11/24/92	9	os	4	75	15.5
40-60	4/14/93	12.3	os	4	7.5	N.A.
40-60	4/14/93	12.3	os	4	15	9.7
40-60	4/14/93	12.3	os	4	22.5	11.6
40-60	4/14/93	12.3	os	4	30	11.4
40-60	4/14/93	12.3	os	4	37.5	10.4
40-60	4/14/93	12.3	os	4	45	N.A.
30-40	04/25/93	0.00312	os	1.33	7.5	N.A.

Large Lysimeter Experimental Results

Size	Date	Rate	Sprinkler Type	Total Amount	Depth	Finger Size
(US Mesh)		(cm/hour)		(cm)	(cm)	(cm)
30-40	04/25/93	0.00312	os	1.33	15	11
30-40	04/25/93	0.00312	os	1.33	17.5	10.7
30-40	04/25/93	0.00312	os	1.33	22.5	11.1
30-40	04/25/93	0.00312	os	1.33	30	10.25
30-40	04/25/93	0.00312	os	1.33	37.5	N.A.

s: disk sprinkler system; os: oscillating sprinkler system

Fig. B-1 (a-h). Large Lysimeter Experimental Results of 14-20 Sand.
(Refer to the results summary on page B-11, 11/20/91)

(a). 7.5 cm depth

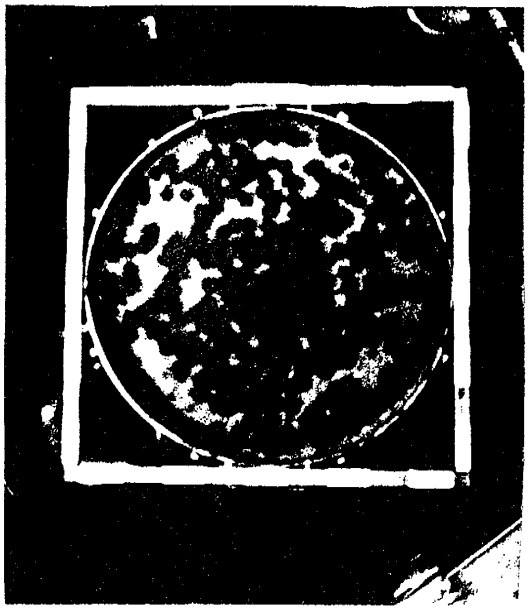

(b). 15 cm depth

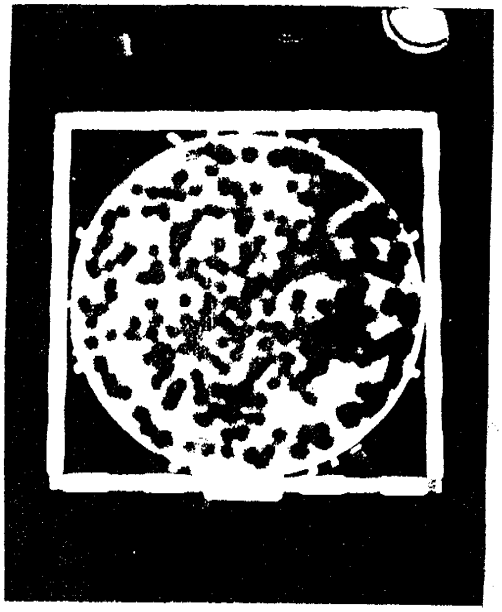

(c). 22.5 cm depth

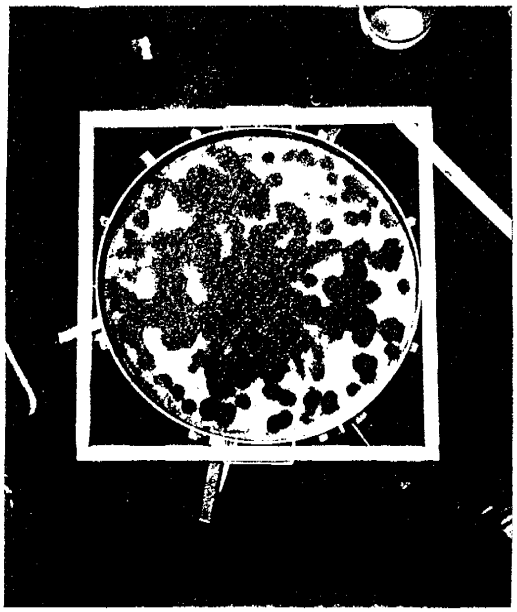

(d). 30 cm depth

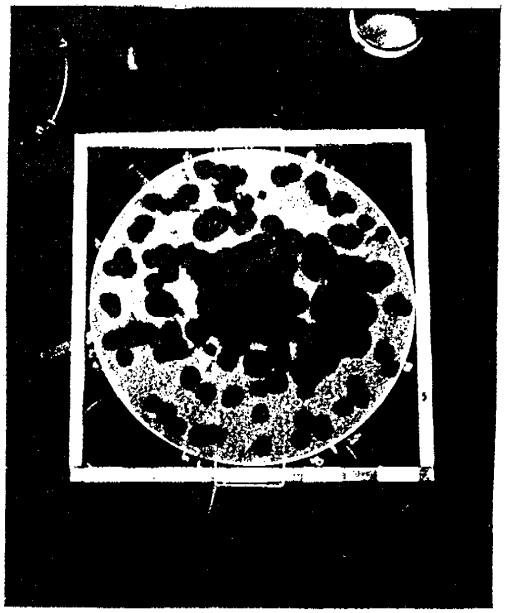

(e). 37.5 cm depth

(f). 45 cm depth

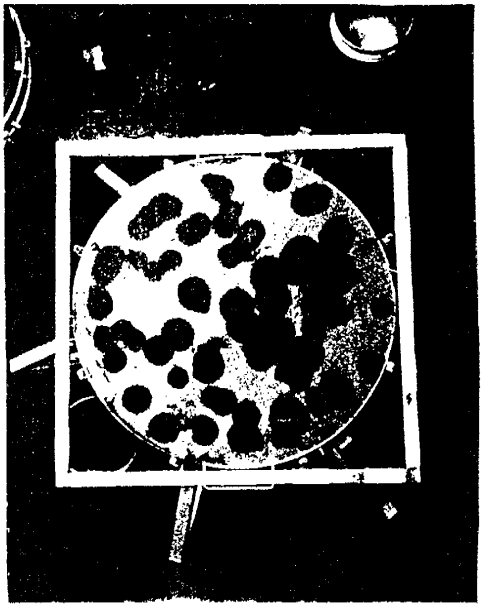

(g). 52.5 cm depth

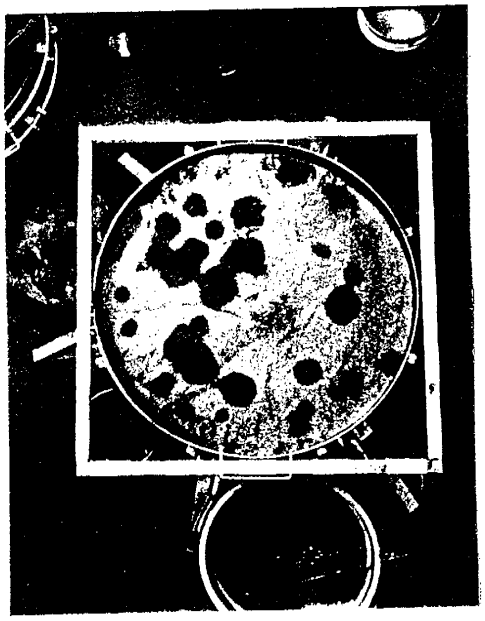

(h). 60 cm depth

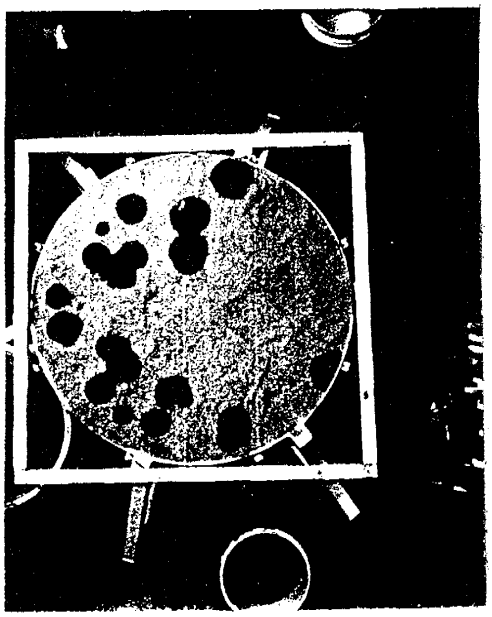

Fig. B-2 (a-j). Large Lysimeter Experimental Results of 30-40 Sand.
(Refer to the results summary on page B-11, 11/24/92)

(a). 7.5 cm depth

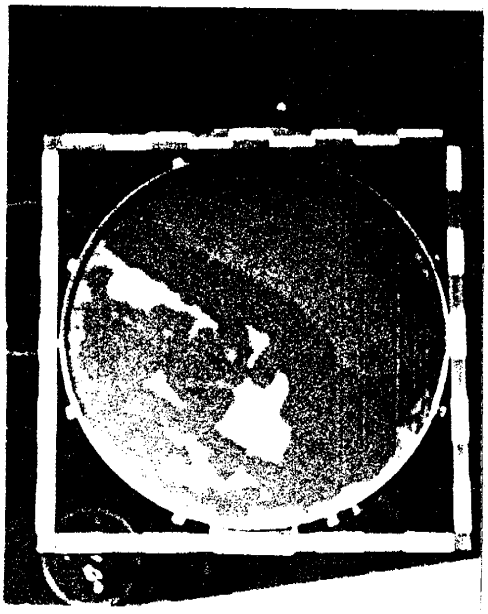

(b). 15 cm depth

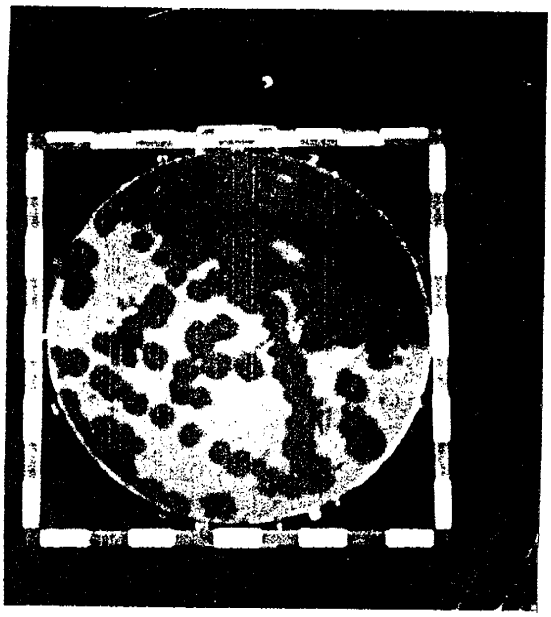

(c). 22.5 cm depth

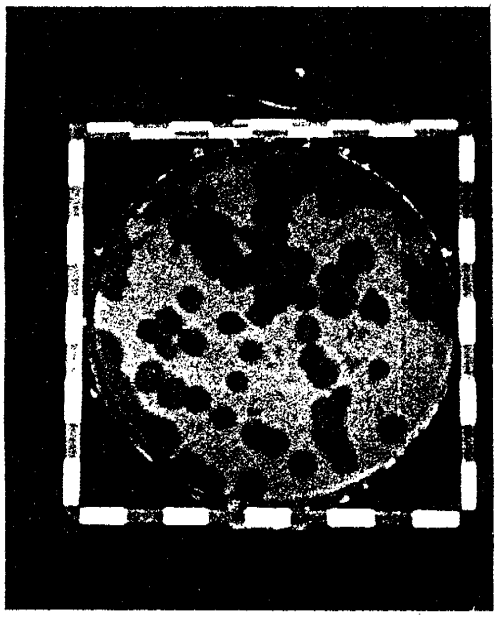

(d). 30 cm depth

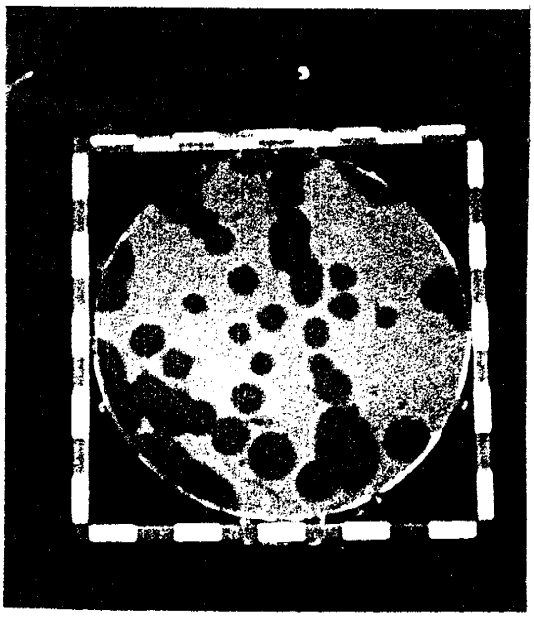

(e). 37.5 cm depth

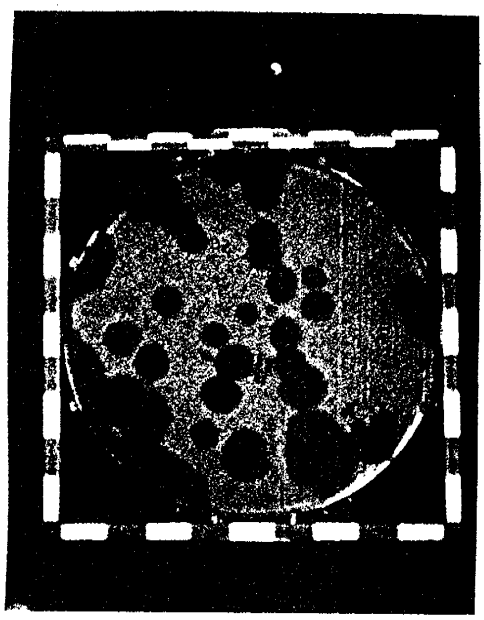

(f). 45 cm depth

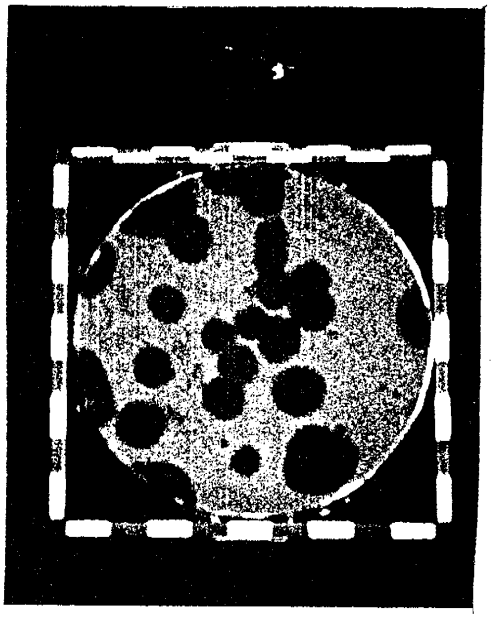

(g). 52.5 cm depth

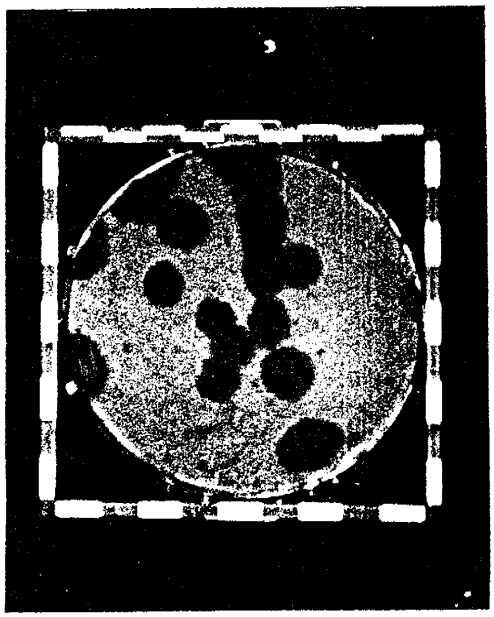

(h). 60 cm depth

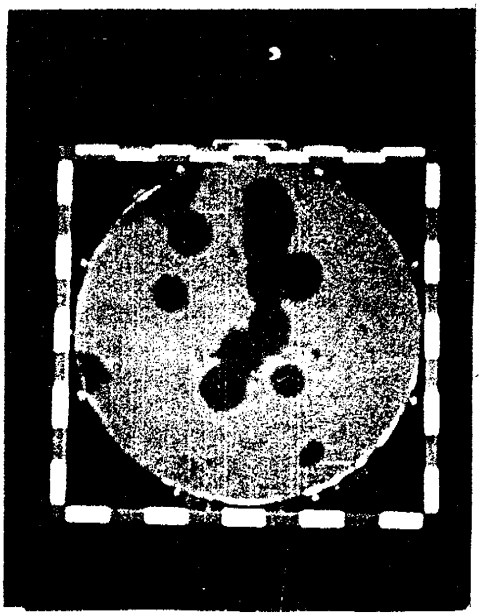

(i). 67.5 cm depth

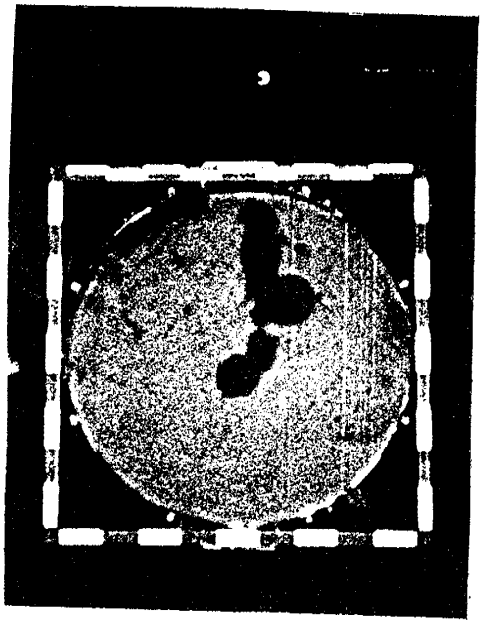

(j). 75 cm depth

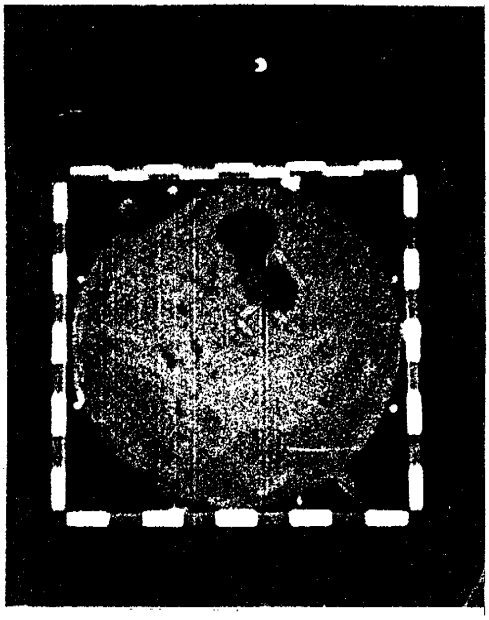

Fig. B-3 (a-f). Large Lysimeter Experimental Results of 40-60 Sand.
(Refer to the results summary on page B-11, 4/14/93)

(a). 7.5 cm depth

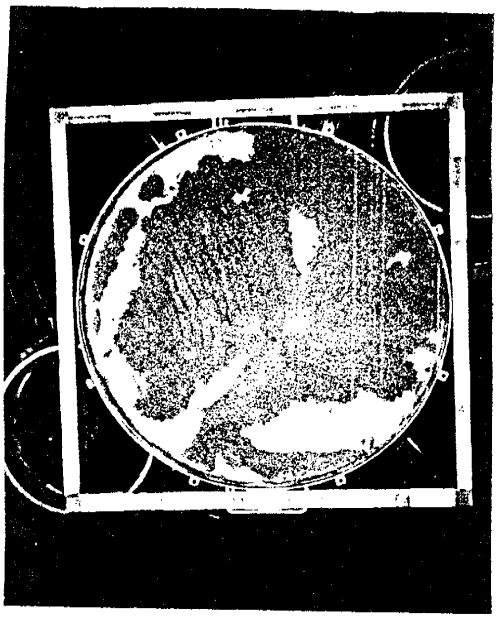

(b). 15 cm depth

(c). 22.5 cm depth

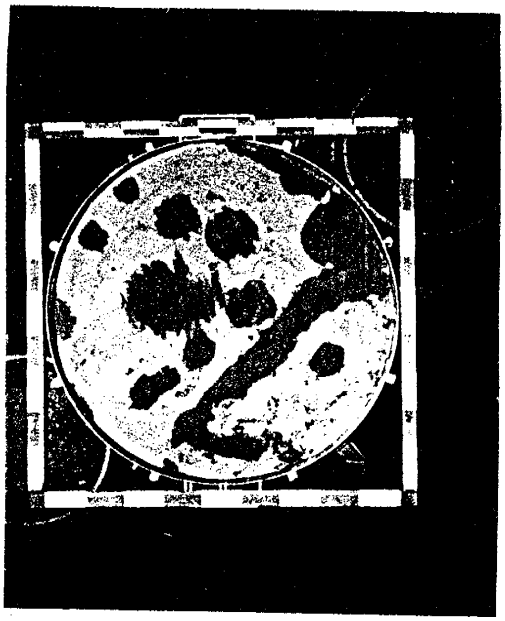

(d). 30 cm depth

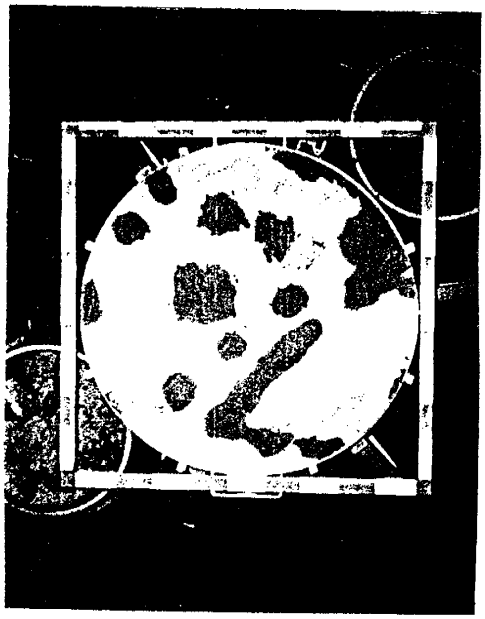

(e). 37.5 cm depth

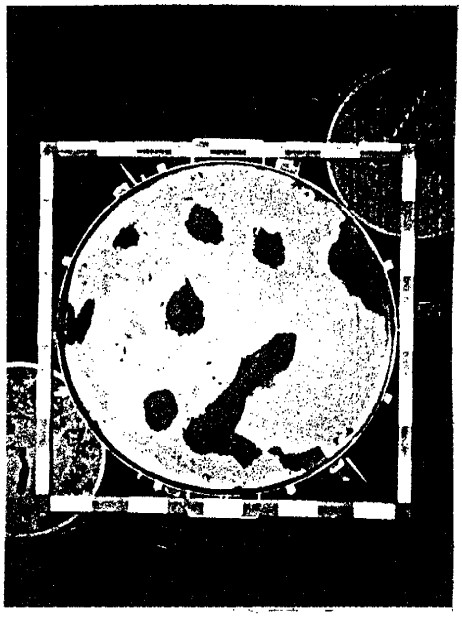

(f). 45 cm depth

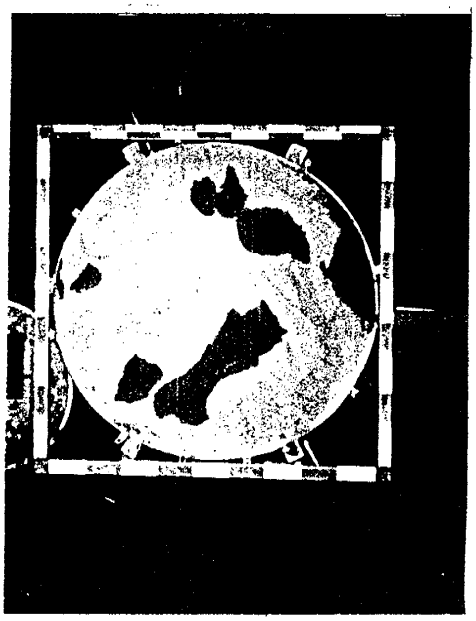

APPENDIX C

SAMPLING RESULTS OF LYSIMETER EXPERIMENTS

APPENDIX C

RESULTS OF LYSIMETER EXPERIMENTS

The gravimetric method was used to determine the water content of the porous medium. The samples were taken destructively from every cross section of our experiments following the measurements and pictures. Each sample ring had a standard 100 cm^3 volume. For the small lysimeter experiments, we took 3-5 samples for each section. For the large lysimeter, 20 samples were taken for each section.

The samples were weighted immediately and dried at 50°C for 24 hours. The samples were then weighed again. The water content was equal to the weight loss divided by 100 cm^3. The bulk densities could also be determined by this set of data (net weight of dry sand/ 100 cm^3). They were in the range of 1.18-1.29 g/cm^3.

The water content inside the fingers and in the wet area could not give us any information during the infiltration process since we took the samples afterward. They served as references for our soil properties.

Tables C-1 and C-2 include two sets of results from the small lysimeter experiments. For different grades of perlite, Table C-1 contains the information for the low infiltration rate experiments and C-2 has the information for the high infiltration rate experiments.

The first digit of the sample number represents the depth of the samples being taken. The numbers 1-5 represent the depths of 0 cm, 10 cm, 20 cm, 30 cm, and 40 cm respectively. The second digit refers to the position of the samples. They were randomly picked for each section.

Table C-1 (a-d). Sampling Results of Low Infiltration Rate Experiments.

(a). 14-20 Sand

Date: 09/23/9 Size: 14-20 Application Rate: .023mm/m

Total Precipitation 50mm

Sam. No	Wet Wt.	Dry Wt.	Water Wt.	Porosity	W. C.	B. Dens.
1-A	129.54	119.81	9.73	0.48768	0.0973	1.1981
1-B	129.1	119.44	9.66	0.48936	0.0966	1.1944
1-C	131.17	131.17	0	0.43605	0	1.3117
1-D	129.78	120.04	9.74	0.48664	0.0974	1.2004
1-E	131.99	122.13	9.86	0.47714	0.0986	1.2213
2-A	132.08	121.44	10.64	0.48027	0.1064	1.2144
2-B	128.11	117.43	10.68	0.4985	0.1068	1.1743
2-C	132.96	121.47	11.49	0.48014	0.1149	1.2147
2-D	126.65	116.83	9.82	0.50123	0.0982	1.1683
2-E	127.87	117.39	10.48	0.49868	0.1048	1.1739
3-A	122.78	118.73	4.05	0.49259	0.0405	1.1873
3-B	129.26	118.06	11.2	0.49564	0.112	1.1806
3-C	131.45	119.72	11.73	0.48809	0.1173	1.1972
3-D	129.24	120.33	8.91	0.48532	0.0891	1.2033
3-E	129.05	118.74	10.31	0.49255	0.1031	1.1874
4-A	119.9	119.71	0.19	0.48814	0.0019	1.1971
4-B	133.68	122.92	10.76	0.47355	0.1076	1.2292
4-C	124.36	124.18	0.18	0.46782	0.0018	1.2418
4-D	132.59	122.95	9.64	0.47341	0.0964	1.2295
4-E	135.14	123.29	11.85	0.47186	0.1185	1.2329
5-A	127.48	124.38	3.1	0.46691	0.031	1.2438
5-B	127.51	125.54	1.97	0.46164	0.0197	1.2554
5-C	137.42	124.69	12.73	0.4655	0.1273	1.2469
5-D	123.08	122.3	0.78	0.47636	0.0078	1.223
5-E	121.73	121.43	0.3	0.48032	0.003	1.2143

(b). 20-30 Sand

Date: 09/23/9 Size: 20-30 Application Rate: .023mm/m

Total Precipitation 50mm

Sam. No	Wet Wt.	Dry Wt.	Water Wt.	Porosity	W. C.	B. Dens.
1-A	132.15	128.98	3.17	0.446	0.0317	1.2898
1-B	129.94	121.2	8.74	0.48136	0.0874	1.212
1-C	132.51	123.18	9.33	0.47236	0.0933	1.2318
1-D	133.74	124.62	9.12	0.46582	0.0912	1.2462
1-E	130.07	121.21	8.86	0.48132	0.0886	1.2121
2-A	136.73	125.72	11.01	0.46082	0.1101	1.2572
2-B	130.08	119.87	10.21	0.48741	0.1021	1.1987
2-C	132.9	122.22	10.68	0.47673	0.1068	1.2222
2-D	125.02	119.41	5.61	0.4895	0.0561	1.1941
2-E	131.29	120.83	10.46	0.48305	0.1046	1.2083
3-A	130.78	120.68	10.1	0.48373	0.101	1.2068
3-B	132.89	121.66	11.23	0.47927	0.1123	1.2166
3-C	134.97	123.49	11.48	0.47095	0.1148	1.2349
3-D	130.52	129	1.52	0.44591	0.0152	1.29
3-E	133.13	121.99	11.14	0.47777	0.1114	1.2199
4-A	127.37	126.95	0.42	0.45523	0.0042	1.2695
4-B	126.86	126.66	0.2	0.45655	0.002	1.2666
4-C	132.9	123.7	9.2	0.47	0.092	1.237
4-D	137.34	125.07	12.27	0.46377	0.1227	1.2507
4-E	131.36	120.18	11.18	0.486	0.1118	1.2018
5-A	126.67	125.17	1.5	0.46332	0.015	1.2517
5-B	129.87	125.12	4.75	0.46355	0.0475	1.2512
5-C	141.96	129.32	12.64	0.44445	0.1264	1.2932
5-D	135.33	123.47	11.86	0.47105	0.1186	1.2347
5-E	132.36	126.29	6.07	0.45823	0.0607	1.2629

(c). 30-40 Sand

Date: 09/23/9 Size: 30-40 Application Rate: .023mm/m

Total Precipitation 50mm

Sam. No	Wet Wt.	Dry Wt.	Water Wt.	Porosity	W. C.	B. Dens.
1-A	129.92	121.76	8.16	0.47882	0.0816	1.2176
1-B	133.55	125.21	8.34	0.46314	0.0834	1.2521
1-C	133.55	125.46	8.09	0.462	0.0809	1.2546
1-D	131.33	123.23	8.1	0.47214	0.081	1.2323
1-E	137.76	129.48	8.28	0.44373	0.0828	1.2948
2-A	135.97	125.47	10.5	0.46195	0.105	1.2547
2-B	132.78	123.18	9.6	0.47236	0.096	1.2318
2-C	131.65	122.5	9.15	0.47545	0.0915	1.225
2-D	138.4	128.34	10.06	0.44891	0.1006	1.2834
2-E	134.17	124.63	9.54	0.46577	0.0954	1.2463
3-A	133.66	123.06	10.6	0.47291	0.106	1.2306
3-B	134.42	124.29	10.13	0.46732	0.1013	1.2429
3-C	137.76	127.32	10.44	0.45355	0.1044	1.2732
3-D	135.31	124.88	10.43	0.46464	0.1043	1.2488
3-E	133.35	122.84	10.51	0.47391	0.1051	1.2284
4-A	127.72	127.6	0.12	0.45227	0.0012	1.276
4-B	127.04	126.89	0.15	0.4555	0.0015	1.2689
4-C	126.81	124.92	1.89	0.46445	0.0189	1.2492
4-D	126.46	126.34	0.12	0.458	0.0012	1.2634
4-E	133.15	124.75	8.4	0.46523	0.084	1.2475
5-A	138.6	120.15	18.45	0.48614	0.1845	1.2015
5-B	141.26	119.04	22.22	0.49118	0.2222	1.1904
5-C	143.61	123.56	20.05	0.47064	0.2005	1.2356
5-D	141.17	122.98	18.19	0.47327	0.1819	1.2298
5-E	138.02	119.49	18.53	0.48914	0.1853	1.1949

(d). 40-60 Sand

Date: 09/23/9 Size: 40-60 Application Rate: .023mm/m

Total Precipitation 50mm

Sam. No	Wet Wt.	Dry Wt.	Water Wt.	Porosity	W. C.	B. Dens.
1-A	137.83	128.74	9.09	0.44709	0.0909	1.2874
1-B	143.36	134.01	9.35	0.42314	0.0935	1.3401
1-C	131.63	122.84	8.79	0.47391	0.0879	1.2284
1-D	136.88	127.86	9.02	0.45109	0.0902	1.2786
1-E	133.27	124.59	8.68	0.46595	0.0868	1.2459
2-A	133.22	123.05	10.17	0.47295	0.1017	1.2305
2-B	139.12	128.6	10.52	0.44773	0.1052	1.286
2-C	134.58	124.44	10.14	0.46664	0.1014	1.2444
2-D	133.01	122.98	10.03	0.47327	0.1003	1.2298
2-E	127.99	118.36	9.63	0.49427	0.0963	1.1836
3-A	132.46	121.14	11.32	0.48164	0.1132	1.2114
3-B	129.88	119.5	10.38	0.48909	0.1038	1.195
3-C	134.14	124.13	10.01	0.46805	0.1001	1.2413
3-D	128.83	118.92	9.91	0.49173	0.0991	1.1892
3-E	137.9	126.32	11.58	0.45809	0.1158	1.2632
4-A	141.95	128.51	13.44	0.44814	0.1344	1.2851
4-B	134.42	122.37	12.05	0.47605	0.1205	1.2237
4-C	137.79	126.21	11.58	0.45859	0.1158	1.2621
4-D	134.87	122.53	12.34	0.47532	0.1234	1.2253
4-E	133.11	121.73	11.38	0.47895	0.1138	1.2173
5-A	146.05	123.08	22.97	0.47282	0.2297	1.2308
5-B	149.78	124.61	25.17	0.46586	0.2517	1.2461
5-C	150.8	129.38	21.42	0.44418	0.2142	1.2938
5-D	148.03	123.83	24.2	0.46941	0.242	1.2383
5-E	152.47	125.85	26.62	0.46023	0.2662	1.2585

Table C-2 (a-d). Sampling Results of High Infiltration Rate Experiments.

(a). 14-20 Sand

Date: 09/26/9 Size: 14-20 Application Rate: .53mm/m

Total Precipitation 40mm

Sam. No	Wet Wt.	Dry Wt.	Water Wt.	Porosity	W. C.	B. Dens.
1-A	128.58	120.16	8.42	0.48609	0.0842	1.2016
1-B	131.66	122.94	8.72	0.47345	0.0872	1.2294
1-C	130.75	122.13	8.62	0.47714	0.0862	1.2213
1-D	126.32	117.88	8.44	0.49645	0.0844	1.1788
1-E	129.19	120.62	8.57	0.484	0.0857	1.2062
2-A	124.88	123.45	1.43	0.47114	0.0143	1.2345
2-B	128.73	121.34	7.39	0.48073	0.0739	1.2134
2-C	128.11	121.35	6.76	0.48068	0.0676	1.2135
2-D	123.99	122.57	1.42	0.47514	0.0142	1.2257
2-E	131.94	124.28	7.66	0.46736	0.0766	1.2428
3-A	124.73	124.64	0.09	0.46573	0.0009	1.2464
3-B	127.75	121.64	6.11	0.47936	0.0611	1.2164
3-C	124.45	124.05	0.4	0.46841	0.004	1.2405
3-D	122.46	122.16	0.3	0.477	0.003	1.2216
3-E	127.94	123.5	4.44	0.47091	0.0444	1.235
4-A	131.35	125.94	5.41	0.45982	0.0541	1.2594
4-B	131.4	131.11	0.29	0.43632	0.0029	1.3111
4-C	123.7	122.42	1.28	0.47582	0.0128	1.2242
4-D	129.33	121.59	7.74	0.47959	0.0774	1.2159
4-E	126.54	125.96	0.58	0.45973	0.0058	1.2596
5-A	127	123.99	3.01	0.46868	0.0301	1.2399
5-B	127.65	124.25	3.4	0.4675	0.034	1.2425
5-C	131.46	123.48	7.98	0.471	0.0798	1.2348
5-D	137.45	128.3	9.15	0.44909	0.0915	1.283
5-E	124.61	122.83	1.78	0.47395	0.0178	1.2283

(b). 20-30 Sand

Date: 09/26/9 Size: 20-30 Application Rate: .53mm/m

Total Precipitation 40mm

Sam. No	Wet Wt.	Dry Wt.	Water Wt.	Porosity	W. C.	B. Dens.
1-A	134.4	125.96	8.44	0.45973	0.0844	1.2596
1-B	128.44	120.39	8.05	0.48505	0.0805	1.2039
1-C	131.43	123.19	8.24	0.47232	0.0824	1.2319
1-D	128.89	120.78	8.11	0.48327	0.0811	1.2078
1-E	132.59	124.18	8.41	0.46782	0.0841	1.2418
2-A	132.89	123.64	9.25	0.47027	0.0925	1.2364
2-B	130.3	120.72	9.58	0.48355	0.0958	1.2072
2-C	132.3	123.34	8.96	0.47164	0.0896	1.2334
2-D	137.03	127.7	9.33	0.45182	0.0933	1.277
2-E	130.63	122.54	8.09	0.47527	0.0809	1.2254
3-A	125.87	124.56	1.31	0.46609	0.0131	1.2456
3-B	132.6	123.69	8.91	0.47005	0.0891	1.2369
3-C	133.37	124.37	9	0.46695	0.09	1.2437
3-D	131.05	130.29	0.76	0.44005	0.0076	1.3029
3-E	131.63	126.59	5.04	0.45686	0.0504	1.2659
4-A	125.16	125.02	0.14	0.464	0.0014	1.2502
4-B	129.76	120.93	8.83	0.48259	0.0883	1.2093
4-C	131.45	121.94	9.51	0.478	0.0951	1.2194
4-D	127.57	127.16	0.41	0.45427	0.0041	1.2716
4-E	130.49	129.58	0.91	0.44327	0.0091	1.2958
5-A	134.69	123.55	11.14	0.47068	0.1114	1.2355
5-B	128.21	123.13	5.08	0.47259	0.0508	1.2313
5-C	132.52	121.36	11.16	0.48064	0.1116	1.2136
5-D	128.73	125.64	3.09	0.46118	0.0309	1.2564
5-E	130.9	125.34	5.56	0.46255	0.0556	1.2534

(c). 30-40 Sand

Date: 09/26/9 Size: 30-40 Application Rate: .53mm/m

Total Precipitation 40mm

Sam. No	Wet Wt.	Dry Wt.	Water Wt.	Porosity	W. C.	B. Dens.
1-A	135.22	126.3	8.92	0.45818	0.0892	1.263
1-B	129.11	121.9	7.21	0.47818	0.0721	1.219
1-C	135.2	126.14	9.06	0.45891	0.0906	1.2614
1-D	130.98	122.56	8.42	0.47518	0.0842	1.2256
1-E	126.62	118.8	7.82	0.49227	0.0782	1.188
2-A	127.63	126.92	0.71	0.45536	0.0071	1.2692
2-B	131.76	122.26	9.5	0.47655	0.095	1.2226
2-C	135.78	124.57	11.21	0.46605	0.1121	1.2457
2-D	129.21	125.06	4.15	0.46382	0.0415	1.2506
2-E	136.72	126.6	10.12	0.45682	0.1012	1.266
3-A	127.41	117.65	9.76	0.4975	0.0976	1.1765
3-B	133.92	133.76	0.16	0.42427	0.0016	1.3376
3-C	134.33	125.99	8.34	0.45959	0.0834	1.2599
3-D	135.5	123.82	11.68	0.46945	0.1168	1.2382
3-E	130.45	130.35	0.1	0.43977	0.001	1.3035
4-A	132.06	119.9	12.16	0.48727	0.1216	1.199
4-B	127.79	127.72	0.07	0.45173	0.0007	1.2772
4-C	133.62	121.89	11.73	0.47823	0.1173	1.2189
4-D	135.3	126.39	8.91	0.45777	0.0891	1.2639
4-E	128.91	128.79	0.12	0.44686	0.0012	1.2879
5-A	138.89	121.5	17.39	0.48	0.1739	1.215
5-B	142.4	125.62	16.78	0.46127	0.1678	1.2562
5-C	146.45	128.7	17.75	0.44727	0.1775	1.287
5-D	147.63	128.91	18.72	0.44632	0.1872	1.2891
5-E	141.86	125.74	16.12	0.46073	0.1612	1.2574

(d). 40-60 Sand

Date: 09/26/9 Size: 40-60 Application Rate: .53mm/m

Total Precipitation 40mm

Sam. No	Wet Wt.	Dry Wt.	Water Wt.	Porosity	W. C.	B. Dens.
1-A	134.21	125.87	8.34	0.46014	0.0834	1.2587
1-B	127.82	118.6	9.22	0.49318	0.0922	1.186
1-C	133.14	122.34	10.8	0.47618	0.108	1.2234
1-D	135.21	125.11	10.1	0.46359	0.101	1.2511
1-E	134.25	123.98	10.27	0.46873	0.1027	1.2398
2-A	125.71	116.76	8.95	0.50155	0.0895	1.1676
2-B	132.38	121.49	10.89	0.48005	0.1089	1.2149
2-C	128.6	121.5	7.1	0.48	0.071	1.215
2-D	130.68	126.47	4.21	0.45741	0.0421	1.2647
2-E	136.76	123.9	12.86	0.46909	0.1286	1.239
3-A	123.86	123.85	0.01	0.46932	0.0001	1.2385
3-B	128.52	128.47	0.05	0.44832	0.0005	1.2847
3-C	126.6	126.54	0.06	0.45709	0.0006	1.2654
3-D	129.58	129.49	0.09	0.44368	0.0009	1.2949
3-E	127.37	126.21	1.16	0.45859	0.0116	1.2621
4-A	128.3	127.87	0.43	0.45105	0.0043	1.2787
4-B	129.18	129.15	0.03	0.44523	0.0003	1.2915
4-C	132.36	132.35	0.01	0.43068	0.0001	1.3235
4-D	122.94	121.5	1.44	0.48	0.0144	1.215
4-E	130.05	130.02	0.03	0.44127	0.0003	1.3002

APPENDIX D

SORPTIVITY MEASUREMENTS OF PERLITE SAND

APPENDIX D

SORPTIVITY MEASUREMENTS OF PERLITE SAND

Sorptivity is an important soil parameter which is defined as a measure of the capacity of a soil to absorb water. It also refers to the cumulative infiltration during the first unit of time.

The general vertical infiltration equation of the unsaturated zone is:

$$\frac{\partial \theta}{\partial t} = \frac{\partial}{\partial s}\left(D\frac{\partial \theta}{\partial s}\right) + \frac{\partial}{\partial s}\left(k\frac{\partial z}{\partial s}\right) \ldots\ldots\ldots Eq.\ (D\text{-}1)$$

where θ is the water content, s is the depth of the wetting front, D is the diffusivity, and k is the hydraulic conductivity.

In the early stage of vertical infiltration the influence of $k\partial z/\partial s$ is much smaller than the influence of $D\partial\theta/\partial s$; thus the driving force due to gravity can be disregarded. The equation can be reduced to:

$$\frac{\partial \theta}{\partial t} = \frac{\partial}{\partial s}\left(D\frac{\partial \theta}{\partial s}\right) \ldots\ldots\ldots Eq.\ (D\text{-}2)$$

By applying the Boltzmann transformation $\lambda = st^{1/2}$, this equation can be transformed into an ordinary differential equation.

Since the cumulative infiltration (I) is:

$$I = \int_{s=0}^{\infty} (\theta - \theta_i)\, ds \ldots\ldots\ldots Eq.\ (D\text{-}3)$$

the sorptivity is introduced after the following derivations:

$$I=\int_{s=0}^{\infty}(\theta-\theta_i)\,ds=\int_{\lambda=0}^{\infty}(\theta-\theta_i)\,d\lambda\,t^{1/2}=t^{1/2}\int_{\lambda=0}^{\infty}(\theta-\theta_i)\,d\lambda \quad .....Eq.\ (D\text{-}4)$$

where

$$S=\int_{\lambda=0}^{\infty}(\theta-\theta_i)\,d\lambda \quad .....Eq.\ (D\text{-}5)$$

which leads to

$$I=St^{1/2} \quad .....Eq.\ (D\text{-}6)$$

The sorptivity measurements were taken through the tension infiltrometer (Ankeny, 1988). By following the principle of $S=I/t^{1/2}$ at the outset, the sorptivity was determined from the slope of the plot of I versus $t^{1/2}$. The margin of error of t was within 3 minutes.

Figure D-1 to D-3 show the sorptivity results of three different grades of perlite sand (20-30, 30-40, and 40-60). The tension values inside the infiltrometer were varied in order to obtain a regression curve from the graph of tension versus sorptivity. The sorptivities at the water-entry values for each sand could be estimated from these regression curves.

Figure D-4 to D-6 show the plots of tension versus sorptivity for three grades of perlite sand. The sorptivities of the perlite sand at the water-entry value are shown in Table 2.

The repeat experiments show the great uncertainty of the sorptivity measurements. Table D-1 shows the results of repeat experiments at a tension of -2.3 cm. Even for our fine sand (40-60 mesh), the average sorptivity value is 0.56 $cm/sec^{1/2}$. The standard

deviation reaches the value of 0.075 (Table D-1).

We did not plot the results for 14-20 sand for two reasons: First, since the tension inside the infiltrometer fluctuates, the device can only be accurate to a 1 cm range. The water-entry for 14-20 sand is close to -3.5 cm. High variability will occur in this region. Second, the fingering phenomena occurs at a very shallow depth. This phenomena could decrease the sorptivity value since only part of the porous medium contributes to the absorption process. This effect may result in an underestimating of finger sizes. The sorptivity of 14-20 sand at a tension of -2.3 cm was assumed to be closed to the value at a tension of -3.5 cm. Our experimental results match this speculation.

Figure D-1. Plot of Sorptivity versus Tension, 20-30 Sand.

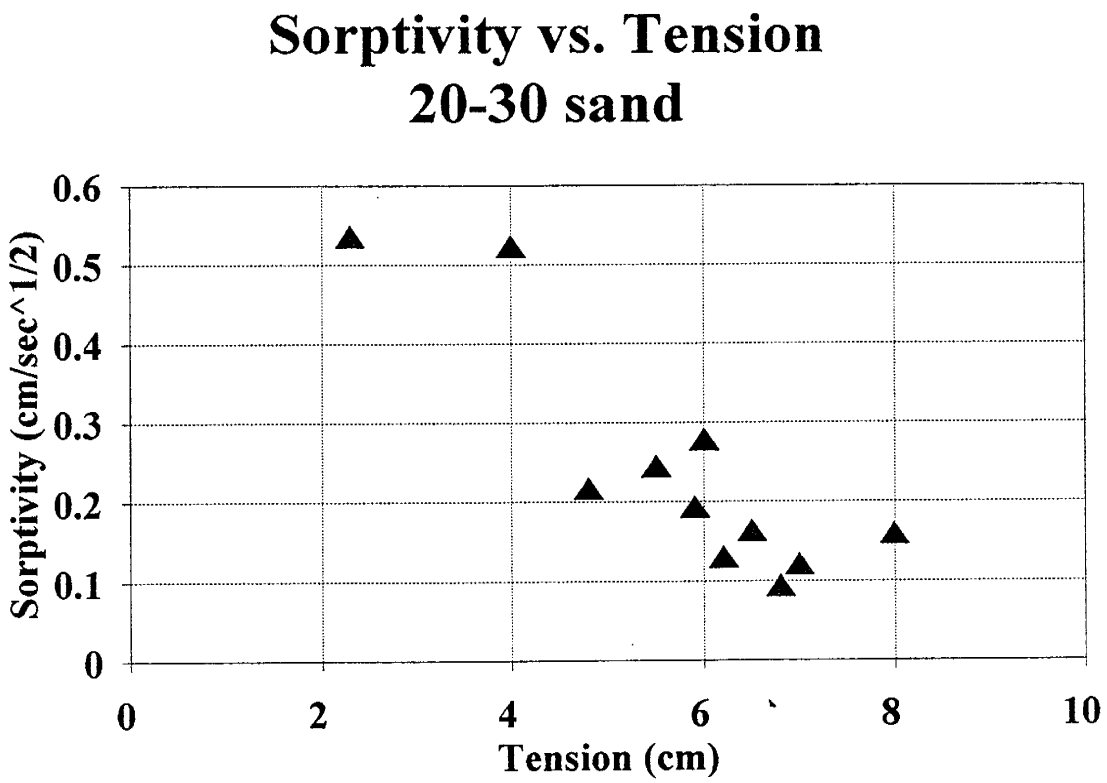

Figure D-2. Plot of Sorptivity versus Tension, 30-40 Sand.

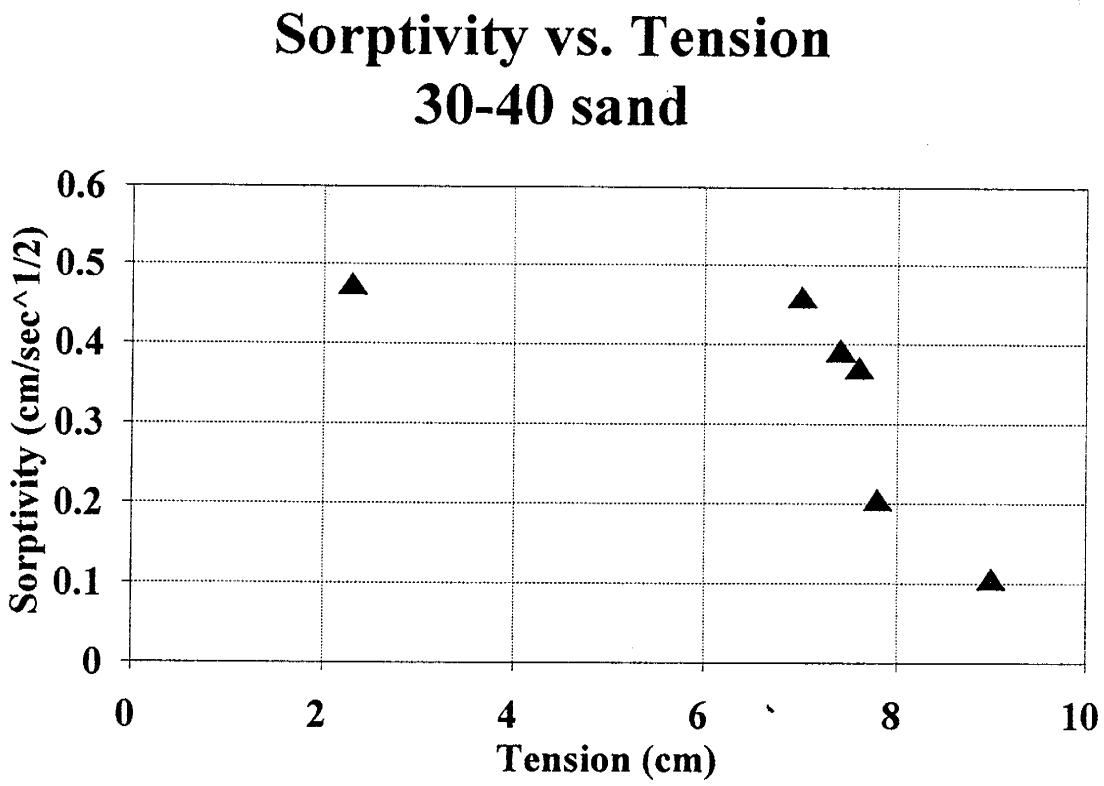

Figure D-3. Plot of Sorptivity versus Tension, 40-60 Sand.

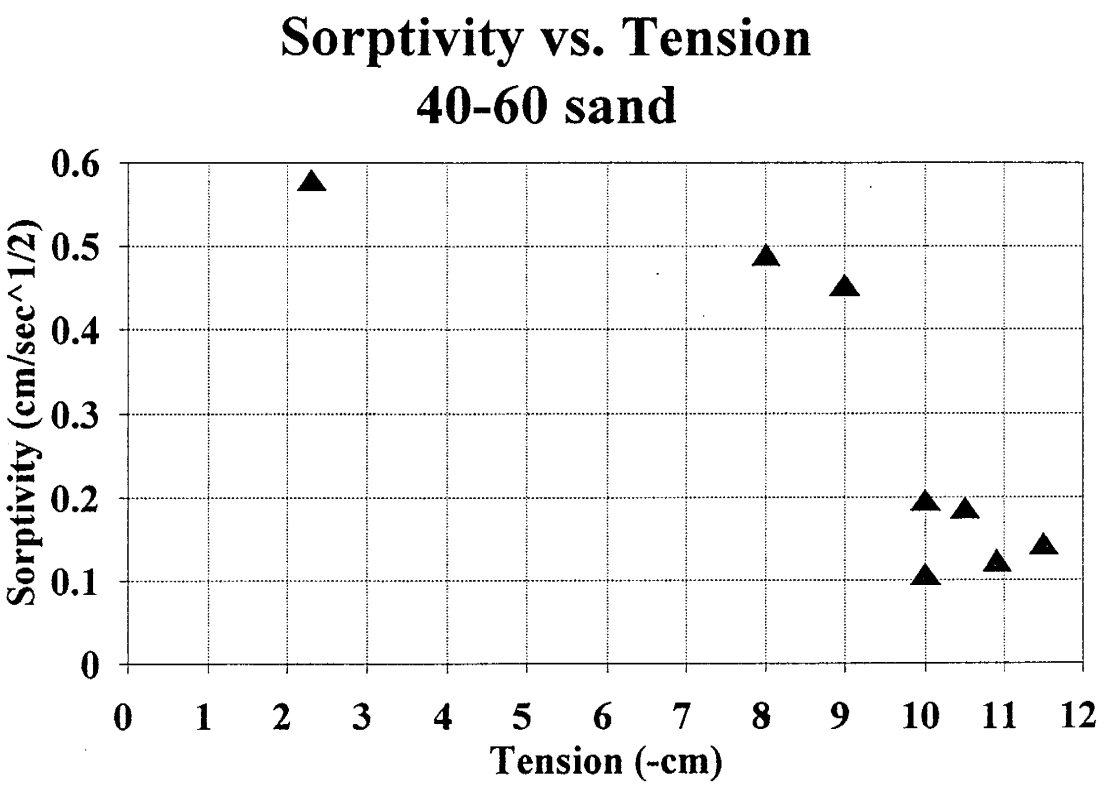

Figure D-4. Plot of Cumulative Infiltration versus Time $^{1/2}$ with Different Tension Values, 20-30 Sand.

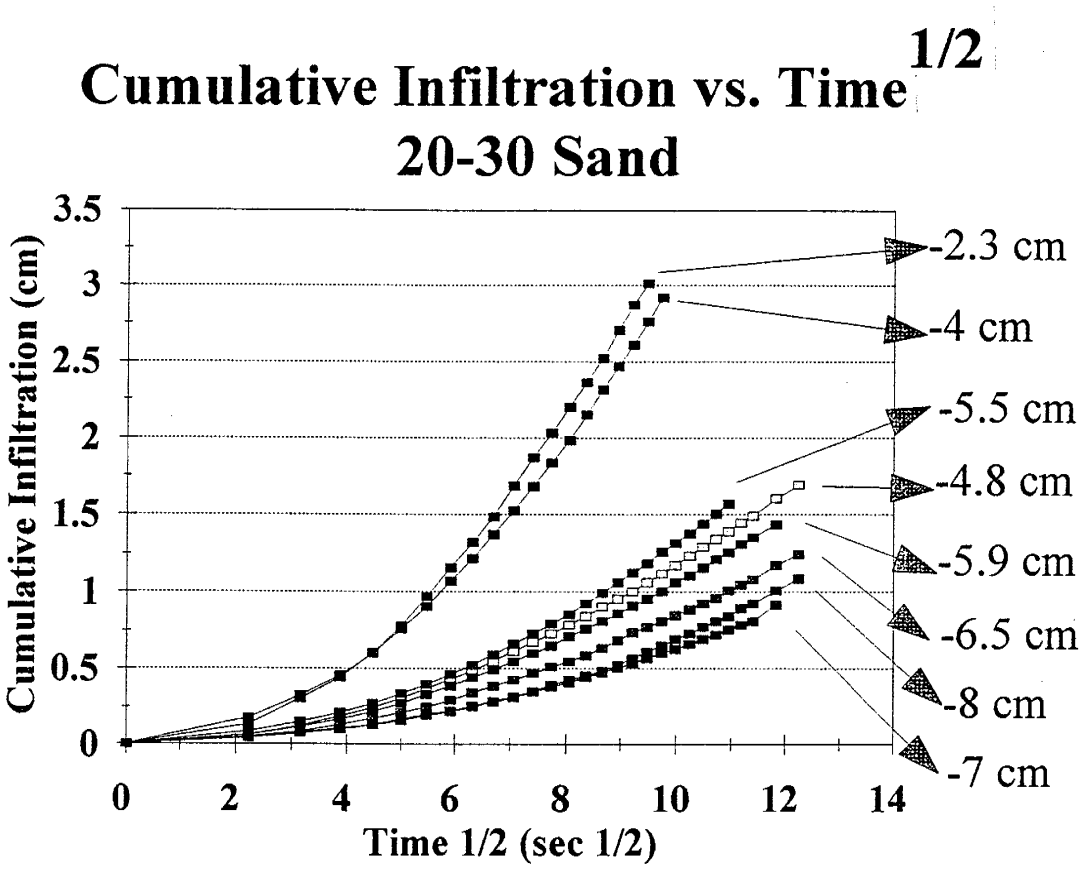

Figure D-5. Plot of Cumulative Infiltration versus Time $^{1/2}$ with Different Tension Values, 30-40 Sand.

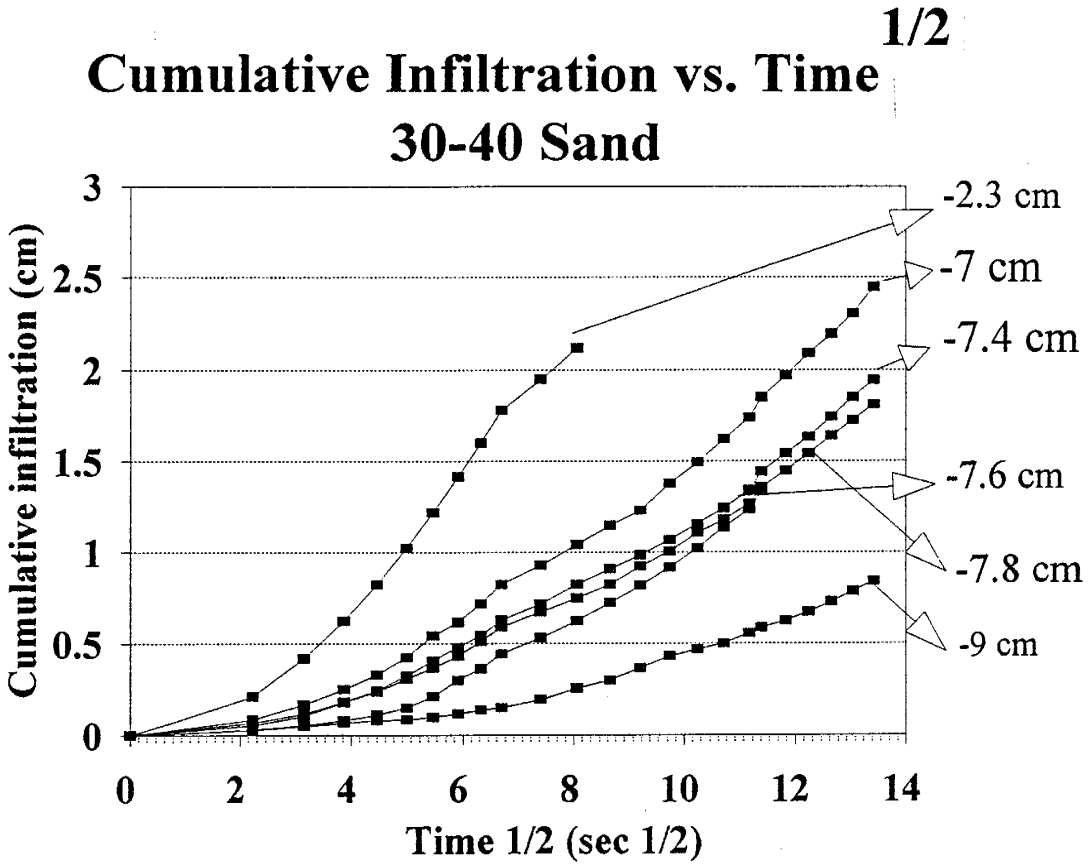

Figure D-6. Plot of Cumulative Infiltration versus Time $^{1/2}$ with Different Tension Values, 40-60 Sand.

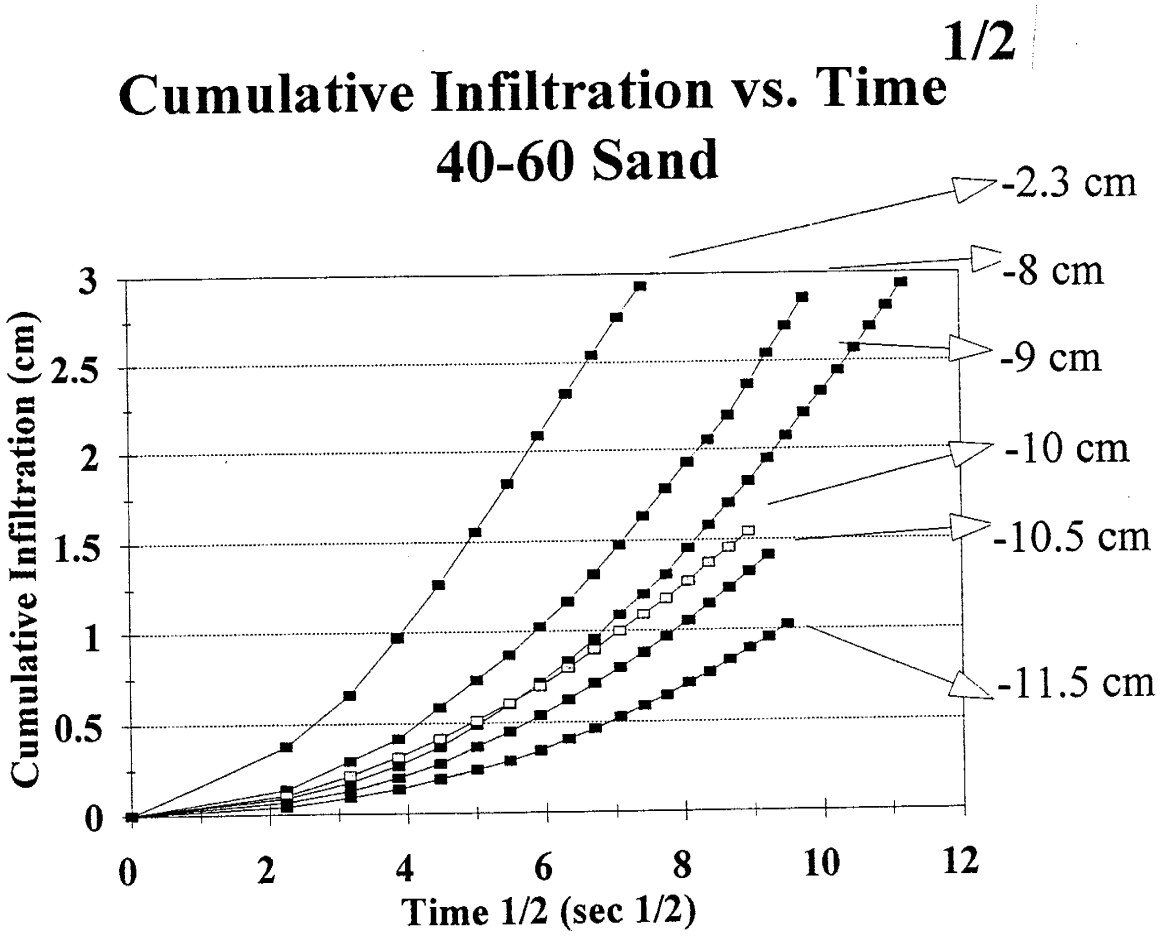

Table D-1. Sorptivity Measurements at the Tension of -2.3 cm.

Exp. No.	14-20	20-30	30-40	40-60
1	0.17	0.51	0.31	0.37
2	0.17	0.53	0.3	0.55
3	0.28	0.62	0.32	0.61
4	0.18	0.52	0.53	0.56
5	0.21	0.51	0.42	0.63
6	0.19	0.55	0.53	0.53
7	0.27	0.51	0.46	0.58
8	0.23	0.43	0.46	0.58
9	0.25	0.37	0.45	0.63
10		0.41		0.57
Average	0.22	0.50	0.42	0.56
Standard Deviation	0.043	0.073	0.09	0.075
Maxima	0.28	0.62	0.53	0.63
Minima	0.17	0.37	0.3	0.37

APPENDIX E

SPRINKLER SYSTEMS

APPENDIX E

SPRINKLER SYSTEMS

Various sprinkler system or rainfall simulators, devices which apply water to research plots in a manner similar to natural rainfall, have been used in our study of unstable wetting fronts.

Basically, we can classify simulators into two groups: the nozzle-type drop formers and the tube-type drop formers. The nozzle-type drop formers produce drops over a wide but uncontrolled range of sizes. In addition the drops are always smaller than the thunderstorm-type of raindrops commonly found in New Mexico. The tube-type drop formers provide more uniform drop sizes but only within a narrow distribution of sizes. The tube-type drop formers ware then chosen as most appropriate.

The disk sprinkler system was first used. Forty-eight tubes were installed on a disk on an area basis. Every tube was designed to cover the same area when it rotated. We used this system in the lab and initially found the uniformity to be satisfactory; however, several defects were eventually discovered: First, dry rings appeared in the central area after we finish applying water for our large lysimeter experiments. This is a natural phenomena of the system since the distance between the tubes increase close to the central area. Second, the tube number was too small for the covered area and intermittency of application occurred; therefore, a new oscillating sprinkler system was designed.

A plexi-glass box was assembled and pre-drilled. In order to simulate high rates of rainfall and cover the area of the large lysimeter, eleven hundred drop formers were

decided to be used. A 20G-1 needle from Becton and Dickinson delivered drop sizes averaging 3 mm in diameter was chosen. The top part of each 1cc syringe was cut and installed in the holes that had been drilled. The needles were then attached to those syringes. The pattern is shown in Fig. E-1.

An oscillating mechanism was chosen, using low gear-motors and moving cams to control the movements. The offset could be adjusted by staggering the rod attachment to the cam. The motor speed could also be varied. By adjusting the offset and varying the speed of the motor, a regular pattern could be avoided. Figure E-2 shows the major parts and some details of this system. The three-frame structure kept this system simple and easy to build.

The uniformity of this system was tested and compared to natural rainfall. During approximately one hour of precipitation, four cm of water was collected through two hundred and fifty-six (16X16) cans. Table E-1 shows the distribution analysis of a rainfall (July 15, 1993) and the simulator. The distribution graphs are shown in Figs. E-3 and E-4.

Based on the results and analysis, the standard variation for natural rainfall and our simulation are very close. The sprinkler system successfully simulates natural rainfall.

Figure E-1. The Drop Formers Pattern of the Oscillating Sprinkler System.

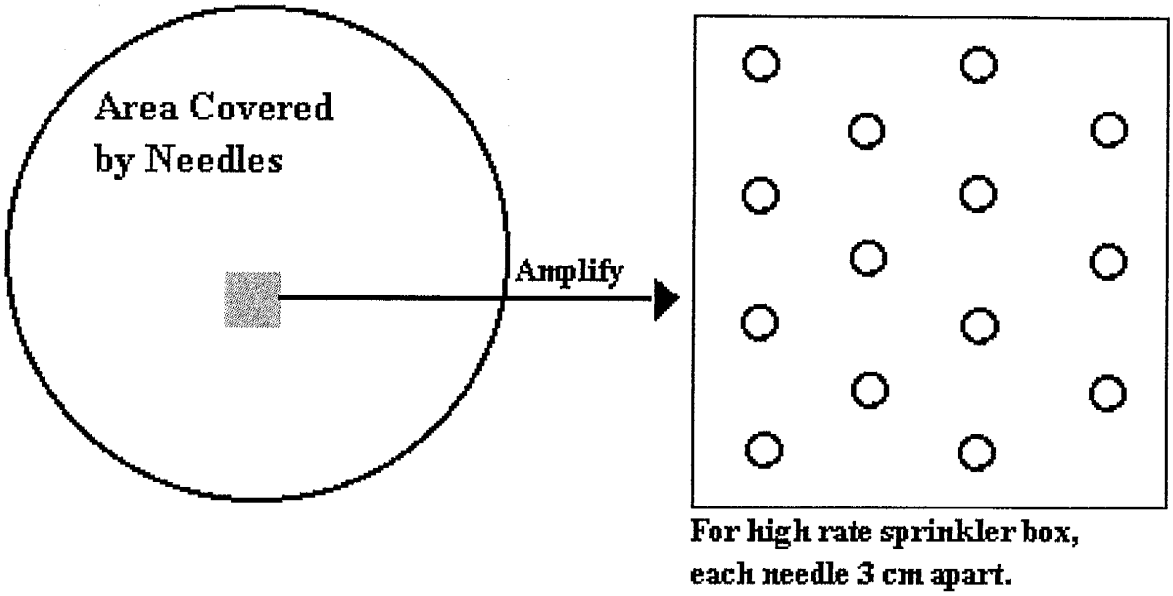

Figure E-2. Design of the Oscillating Sprinkler System.

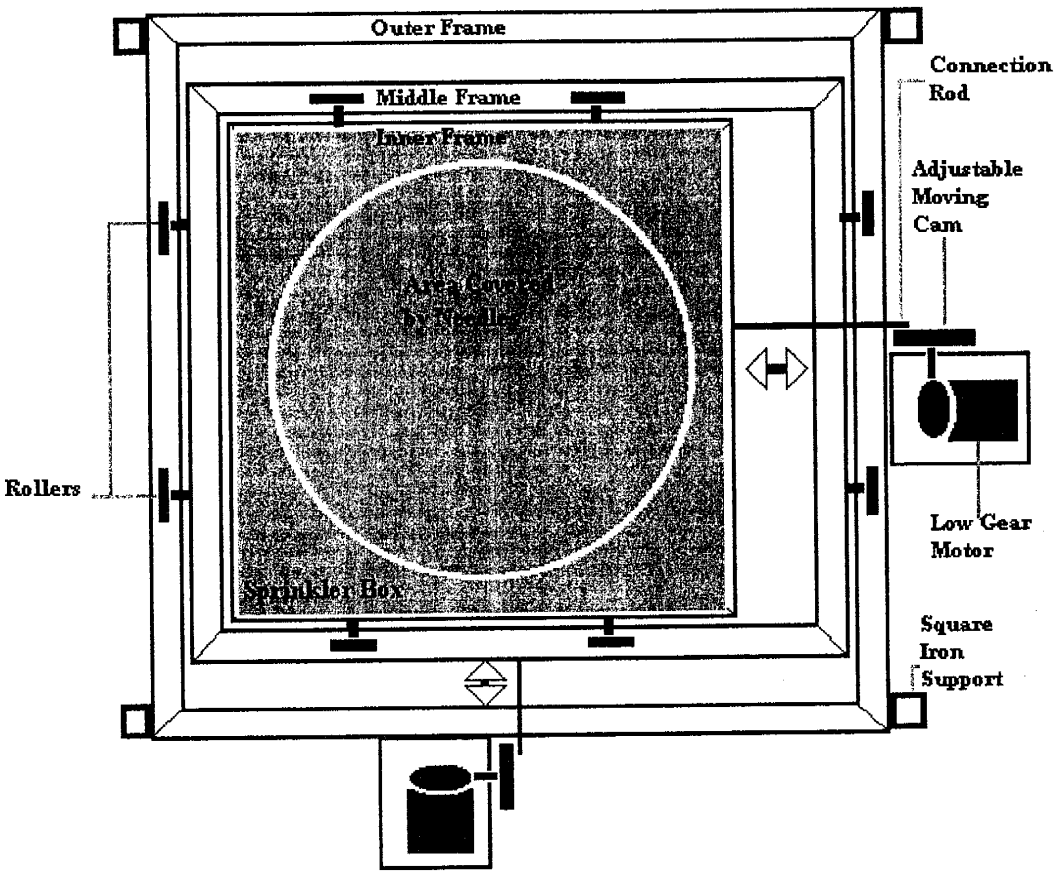

Figure E-3. Distribution Graph of Natural Rain.

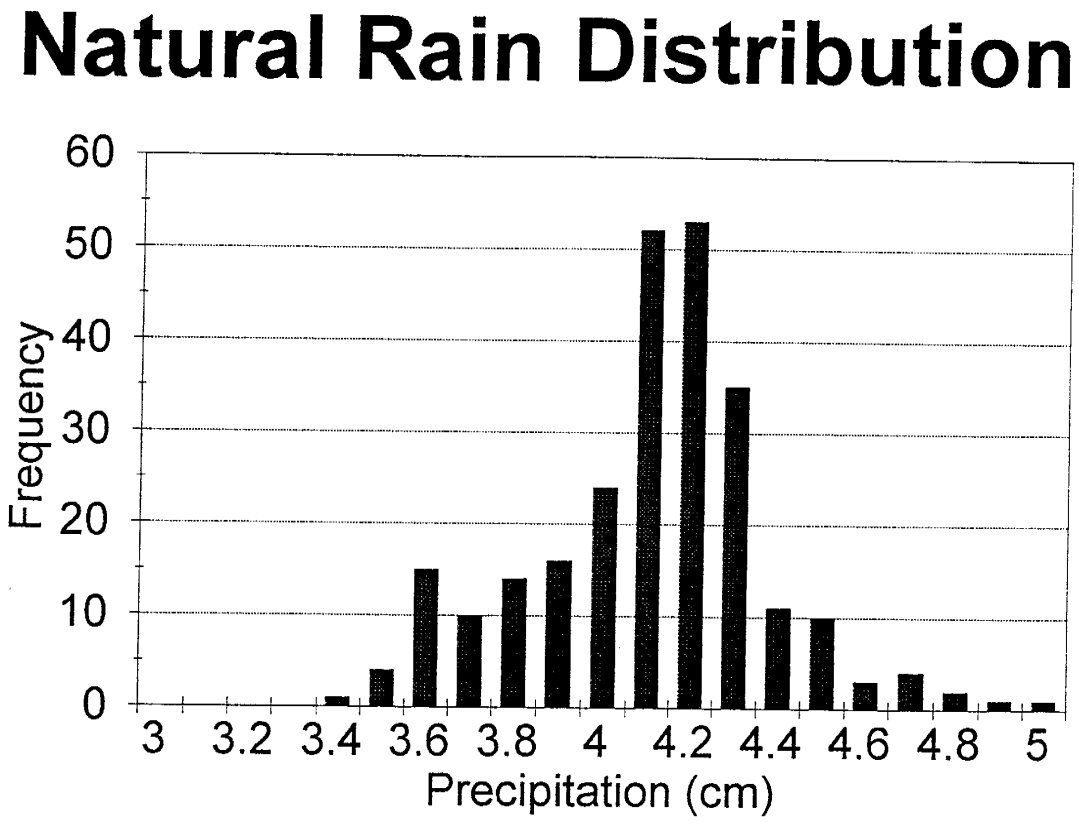

Figure E-4. Distribution Graph of Rain Simulator (Oscillating sprinkler system).

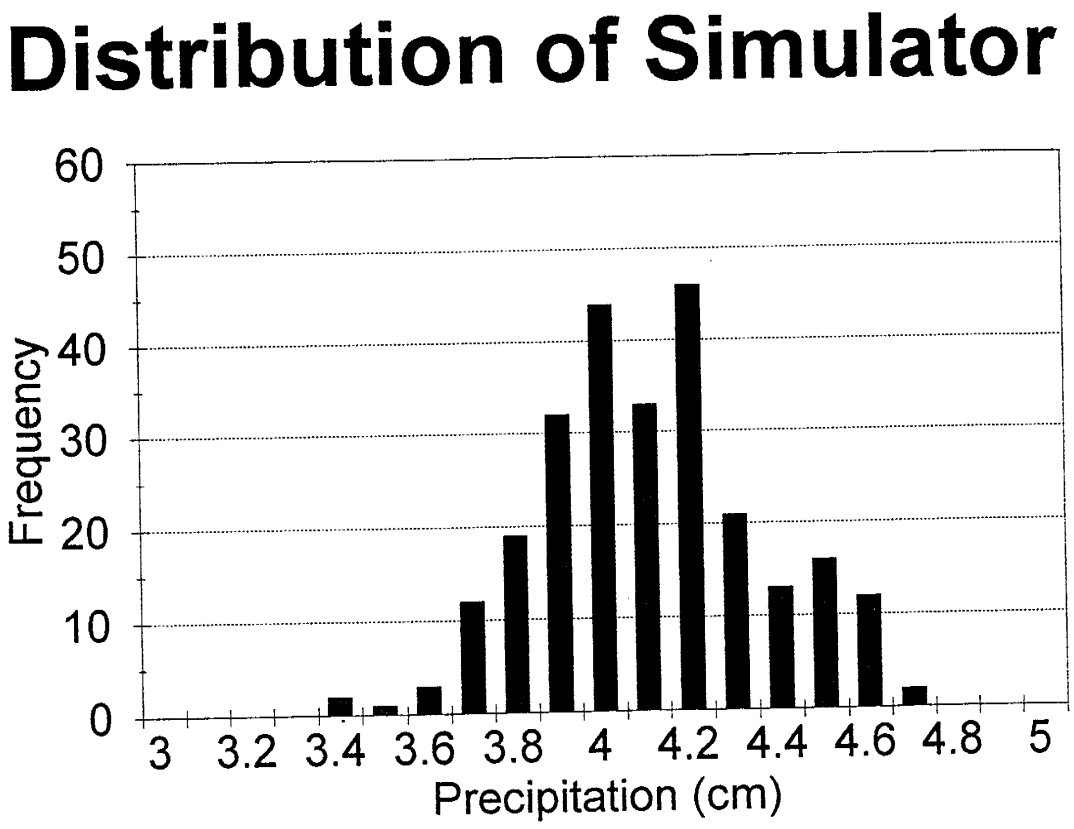

Table E-1. Distribution Analysis of Rainfall and Simulator.

(Precipitation of natural and simulated rainfall are at the average of 4.06cm)

Minima	Data points	Standard Deviation	Variance	Maxima	
				cm	cm
Natural rainfall	256	0.266	0.07	4.93	3.38
Simulator					
Trial 1	64	0.24	0.0578	4.59	3.62
Trial 2	64	0.229	0.0528	4.49	3.57
Trial 3	64	0.31	0.096	4.69	3.32
Trial 4	64	0.242	0.0586	4.57	3.49
Total	256	0.253	0.0635	4.69	3.32